5.5. Coastal and inland waters

SeaWiFS and MODIS Experiences Show:

High quality ocean color products for the global open oceans (Case-1 waters).

Significant efforts are needed for improvements of water color products in the inland & coastal regions:

- **Turbid Waters**
  (violation of the NIR black ocean assumption)
- **Strongly-Absorbing Aerosols**
  (violation of non- or weakly absorbing aerosols)

Algorithm Developments for Productive/Turbid Waters

- **Arnone** et al. (1998) and **Siegel** et al. (2000) to account for the NIR ocean contributions for SeaWiFS and MODIS NIR bands.
- **Hu** et al. (1999) proposed an *adjacent pixel method*.
- **Gordon** et al. (1997) and **Chomko** et al. (2003) *the spectral optimization algorithm*.
- **Ruddick** et al. (2000) for regional Case-2 algorithm using the *spatial homogeneity of the aerosol* in a given area.
- **Lavender** et al. (2004) regional bio-optical model (suspended sediments) for SeaWiFS application.
- **Wang** and **Shi** (2005) derived NIR ocean contributions using the MODIS shortwave infrared (**SWIR**) bands.
- **Doerffer** et al. and others developed Artificial *Neural Network* for coastal Case-2 waters (implemented for MERIS data processing).
- **Wang** (2007) and **Wang** & **Shi** (2007) proposed the SWIR and NIR-SWIR atmospheric correction for the coastal waters.
- **Bailey** et al. (2010) developed an improved NIR model for the NASA standard ocean color data processing (SeaDAS).
- **Wang** et al. (2012) developed an NIR model for western Pacific regions (highly turbid) using the data from the SWIR algorithm for GOCI sensor.

The NIR Ocean Contribution Modeling (I)

Various investigators all sought to remove the NIR $nL_w(\lambda)$ contributions from the TOA NIR radiances, so that a "**black pixel**" could be provided to the *Gordon and Wang* (1994) type atmospheric correction:

- **Siegel** et al. (2000) used chlorophyll estimate to determine the NIR $nL_w(\lambda)$.
- **Lavender** et al. (2005) used a sediment estimate to determine the NIR $nL_w(\lambda)$.
- **Ruddick** et al. (2000) fixed the aerosol and backscatter type and then solved for both the NIR $nL_w(\lambda)$ and NIR aerosol reflectance simultaneously.
- **Arnone** et al. (1998) and **Stumpf** et al. (2003) used a bio-optical model for absorption coefficient at the red band and then used that with the red $nL_w(\lambda)$ to find the NIR $nL_w(\lambda)$.
- **Bailey** et al. (2010) developed an improved NIR model for the NASA standard ocean color data processing (SeaDAS).
- **Wang** et al. (2012) developed an NIR model for western Pacific regions (highly turbid) using the data from the SWIR algorithm for GOCI sensor.

The NIR Ocean Contributions Modeling (Example 1)
(Siegel et al., 2000)

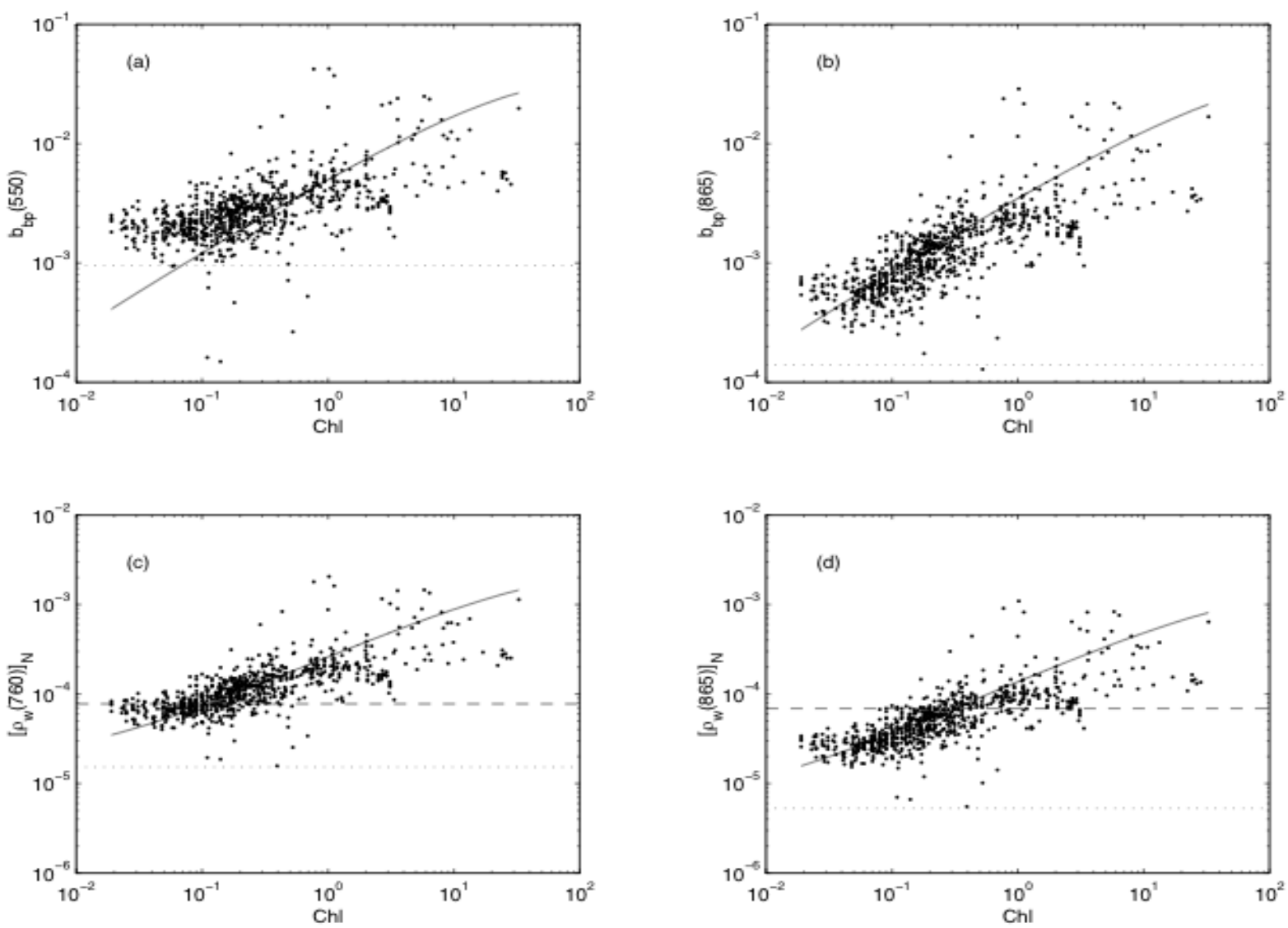

The NIR Ocean Contributions Modeling (Example 1)

(Siegel et al., 2000)

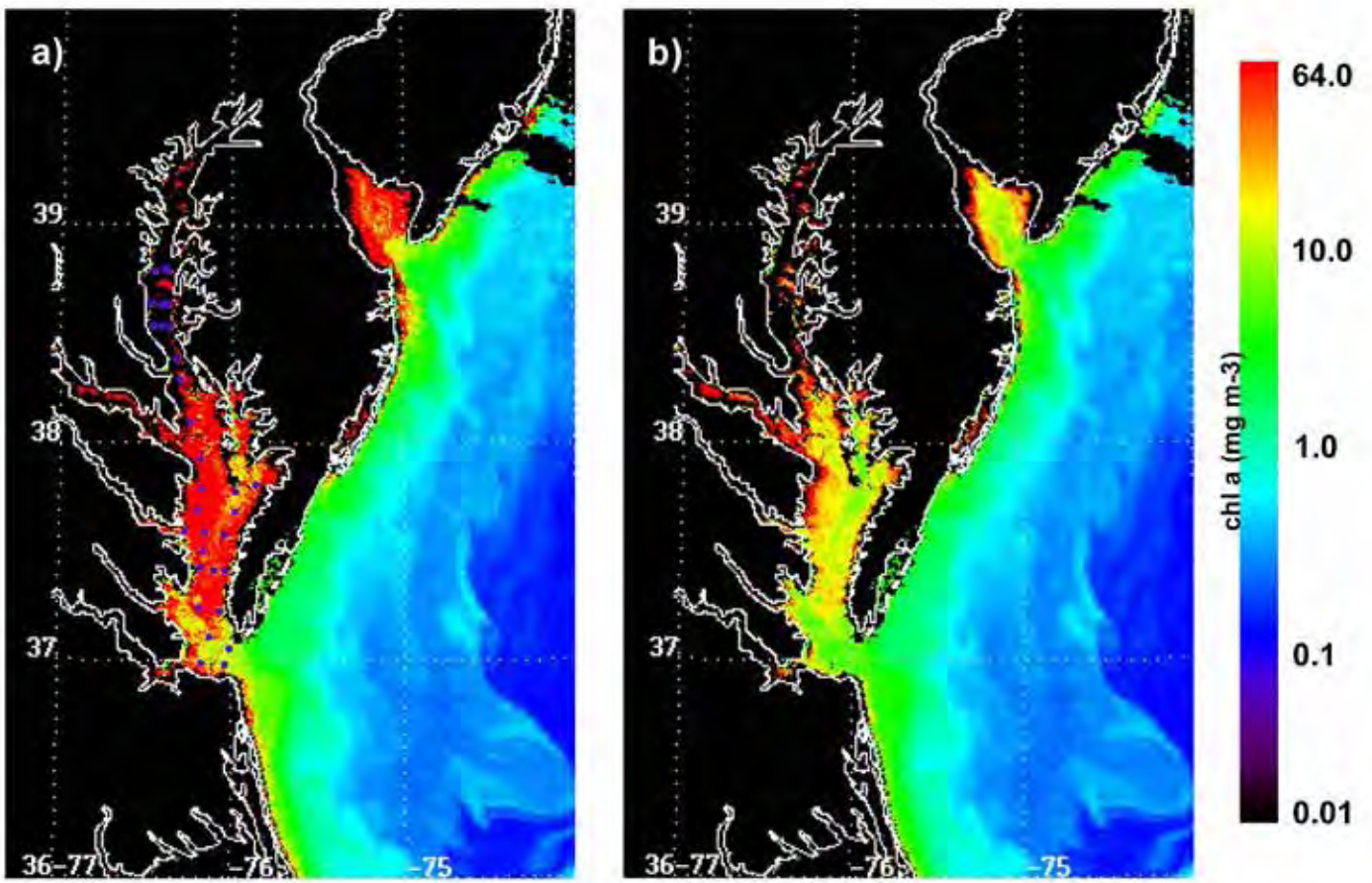

NASA Std

Siegel et al. (2000)

Red-NIR Ocean Reflectance vs. SPM

The NIR Ocean Contributions Modeling (Example 2)

(Lavender et al., 2000)

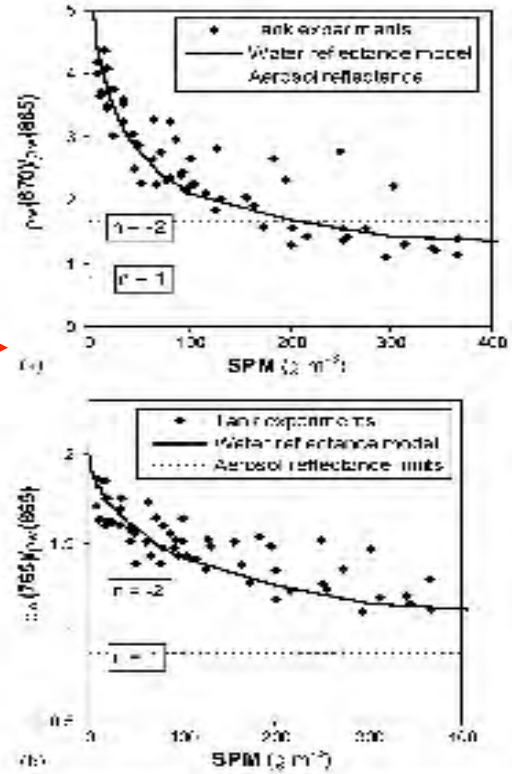

Fig. 2. Water reflectance and aerosol reflectance ratios in the NIR, shown as a function of the SPM parameter. (a) The ratio between the 670 and 865 nm bands. (b) The ratio between the 765 and 865 nm bands. The line shows the model developed to represent water reflectance when dominated by SPM. The aerosol reflectance ratios may lie anywhere region bounded by the dashed lines representing Ångström exponents (n) of +1 to −2. The optical signature of the water and aerosol are indistinguishable where the water reflectance ratios lie between these lines.

largely determines water reflectance in the majority of SPM dominated natural waters. This decision is arbitrary. Actual total SPM concentration will tend to be greater than the model SPM parameter by an amount that depends on the particle size distribution of the particular sediment: the finer the sediment and the smaller the difference.

Absorption and backscatter by SPM in the model were taken as Eqs (6) and (7) respectively. Note that the model is only applicable to the range $0.1 < \mathrm{SPM} < 200\ \mathrm{g\,m^{-3}}$.

$$a_{\mathrm{SPM}}(\lambda) = a^*_{\mathrm{SPM}}(\lambda)\mathrm{SPM}^{0.32}, \tag{6}$$

$$b_{\mathrm{SPM}}(\lambda) = 0.85\,\mathrm{SPM}\left(\frac{\lambda}{670}\right)^{-0.9}, \tag{7}$$

where the empirical constants are: $a^*_{\mathrm{SPM}}(\lambda) = [0.65, 0.45, 0.12]$ for $\lambda = [670, 765, 865]$ respectively. A radiative transfer model, Hydrolight (Mobley, 1995), was used to obtain water reflectance from these absorption and scattering values for various sun positions and satellite viewing geometries. Pure water absorption data were taken from Pope and Fry (1997) and Palmer and Williams (1974), water scattering data were taken from Morel (1974), and the SPM scattering phase function of Petzold (1972) was used. The model results are shown in Figs. 1 and 2. The results were incorporated into a look-up table for use in the BP atmospheric correction method.

2.3. The Bright Pixel inversion model

The method used to partition the Rayleigh-corrected reflectance into aerosol and water reflectance is similar to that employed by the European MERIS satellite sensor (Moore et al., 1999), see Fig. 3 for an overview of the scheme. The MERIS method uses the NIR bands centred on 705, 775 and 865 nm, whereas the SeaWiFS method described here uses the 670, 765 and 865 nm bands. The significance of this band change is considered later.

Neglecting the effects of phytoplankton and CDOM on NIR reflectance, Eqs (3) and (5) give:

$$\begin{aligned}\rho_{rc}(\lambda) &= \rho_r(\lambda) - \rho_a(\lambda)\\ &= \rho'_a + t(\lambda) f(\lambda, \mathrm{SPM}, \theta_0, \theta, \phi).\end{aligned} \tag{8}$$

Combining Eqs. (4) and (8) we can express the Rayleigh-corrected top-of-atmosphere reflectance (ρ_{rc}) at 670 and 765 nm as two non-linear linked equations:

$$\begin{aligned}\rho_{rc}(670) = \rho'_a(865)\left(\frac{670}{865}\right)^n\\ + t(670) f(670, \mathrm{SPM}, \theta_0, \theta, \phi),\end{aligned} \tag{9}$$

Spectral Optimization Algorithm (II)

- The **Spectral Optimization Algorithm (SOA)** (Chomko and Gordon, 1998) derives the properties of the ocean and atmosphere simultaneously using sensor-measured TOA radiance from the blue to NIR (entire radiance spectra from visible to NIR). However, the algorithm has no attempt to use **realistic aerosol models**.
  - Use a simple power-law size distribution aerosol model
  - Use the Garver-Siegel-Maritorena (GSM) ocean bio-optical model
  - Some studies with SeaWiFS data show improved results over the coastal productive waters (Kuchinke et al., 2009).

✓ The SOA approach with simultaneously ocean and atmosphere properties retrieval (one-step) requires **robust ocean bio-optical model** (e.g., over complex turbid waters).

Example Results of SOA (Chl-a)

(*Kuchinke et al.*, 2009)

SOA+GSM

Std+GSM

NASA Std

Images Left to Right:
22 Jul 1998, 11 Aug 1998, and 26 Jun 1999

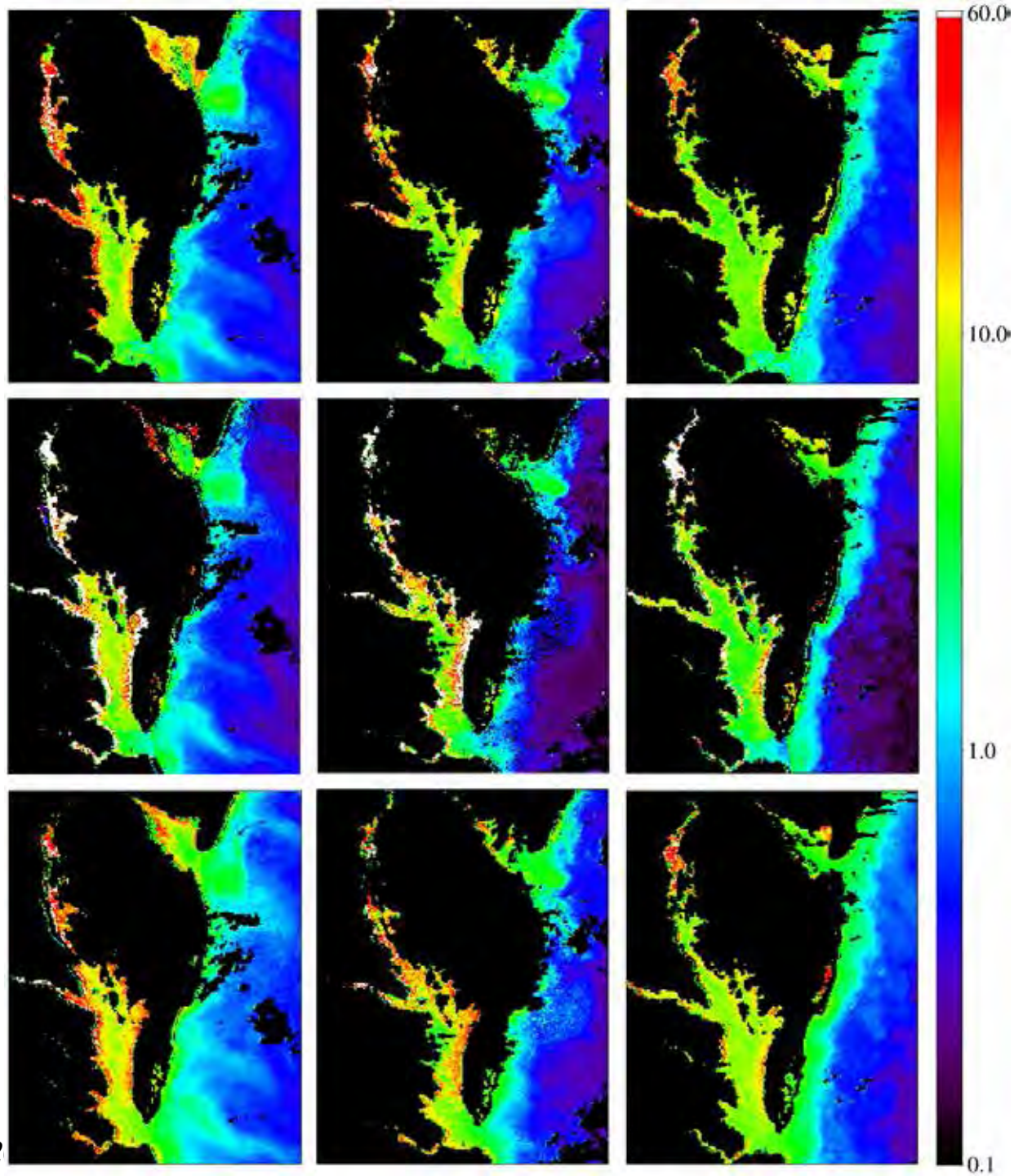

(III)

Atmospheric correction based on modelled radiance reflectances and artificial neural network

International Ocean Color Workshop Agenda
(23-24 April. 2009, Hangzhou, China)

R. Doerffer, GKSS
Institute for Coastal Research

GKSS

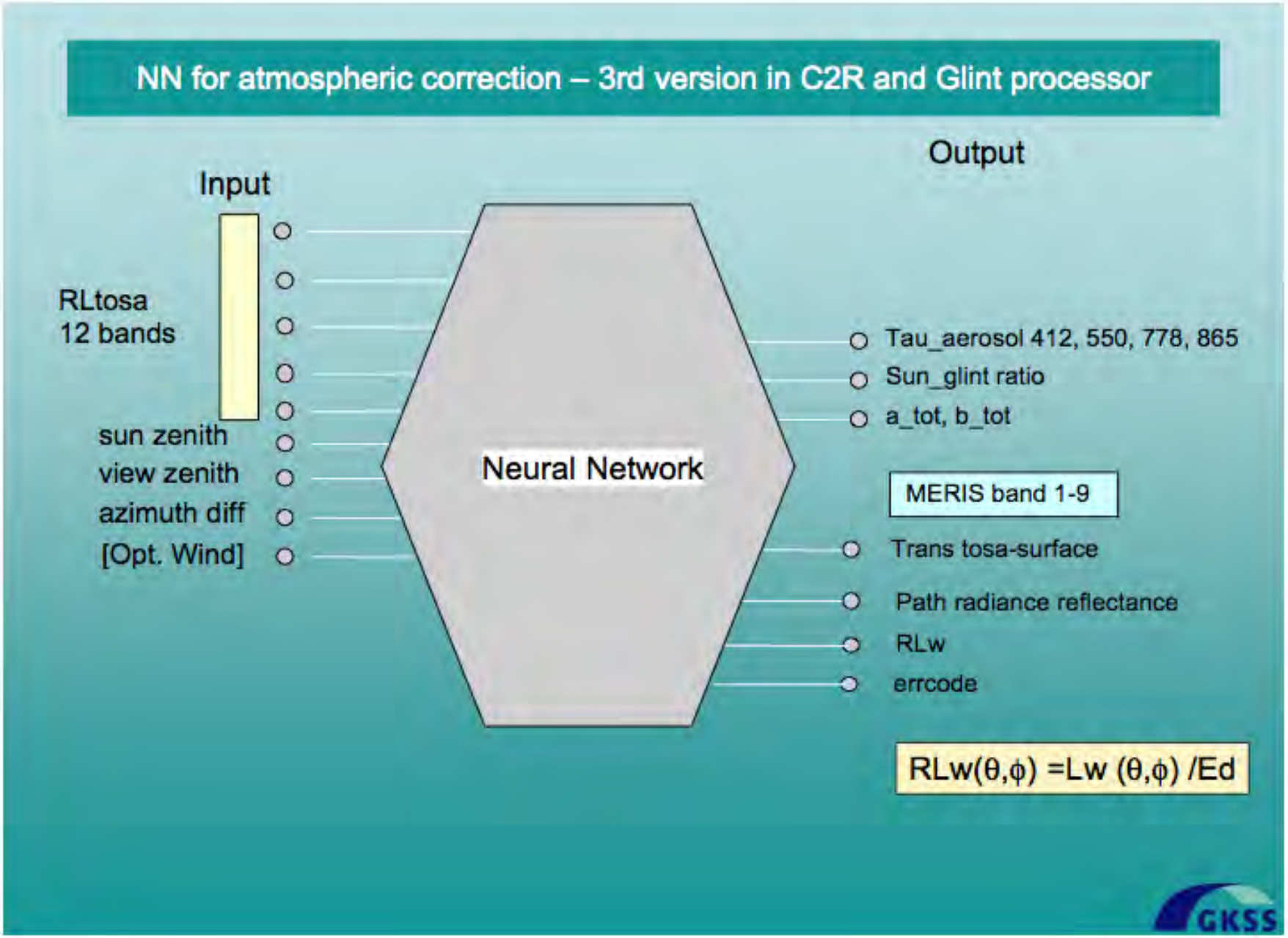

From R. Doerffer

Atmospheric Correction: SWIR Bands

(Wang & Shi, 2005; Wang, 2007)

- At the shortwave IR (SWIR) wavelengths (>~1000 nm), ocean water has much strongly absorption and ocean contributions are significantly less. Thus, atmospheric correction can be carried out for coastal regions **without using the bio-optical model**.
- Water absorption for 869 nm, 1240 nm, 1640 nm, and 2130 nm are 5 m^{-1}, 88 m^{-1}, 498 m^{-1}, and 2200 m^{-1}, respectively.
- Examples using the MODIS Aqua **1240** and **2130 nm** data to derive the ocean color products are provided.

➢ We use the SWIR band (1240 nm) for the cloud masking. This is necessary for coastal region waters.

✓ Require sufficient **SNR** characteristics for the SWIR bands and the SWIR atmospheric correction has slight larger noises at the short visible bands (compared with those from the NIR algorithm).

Water Absorption

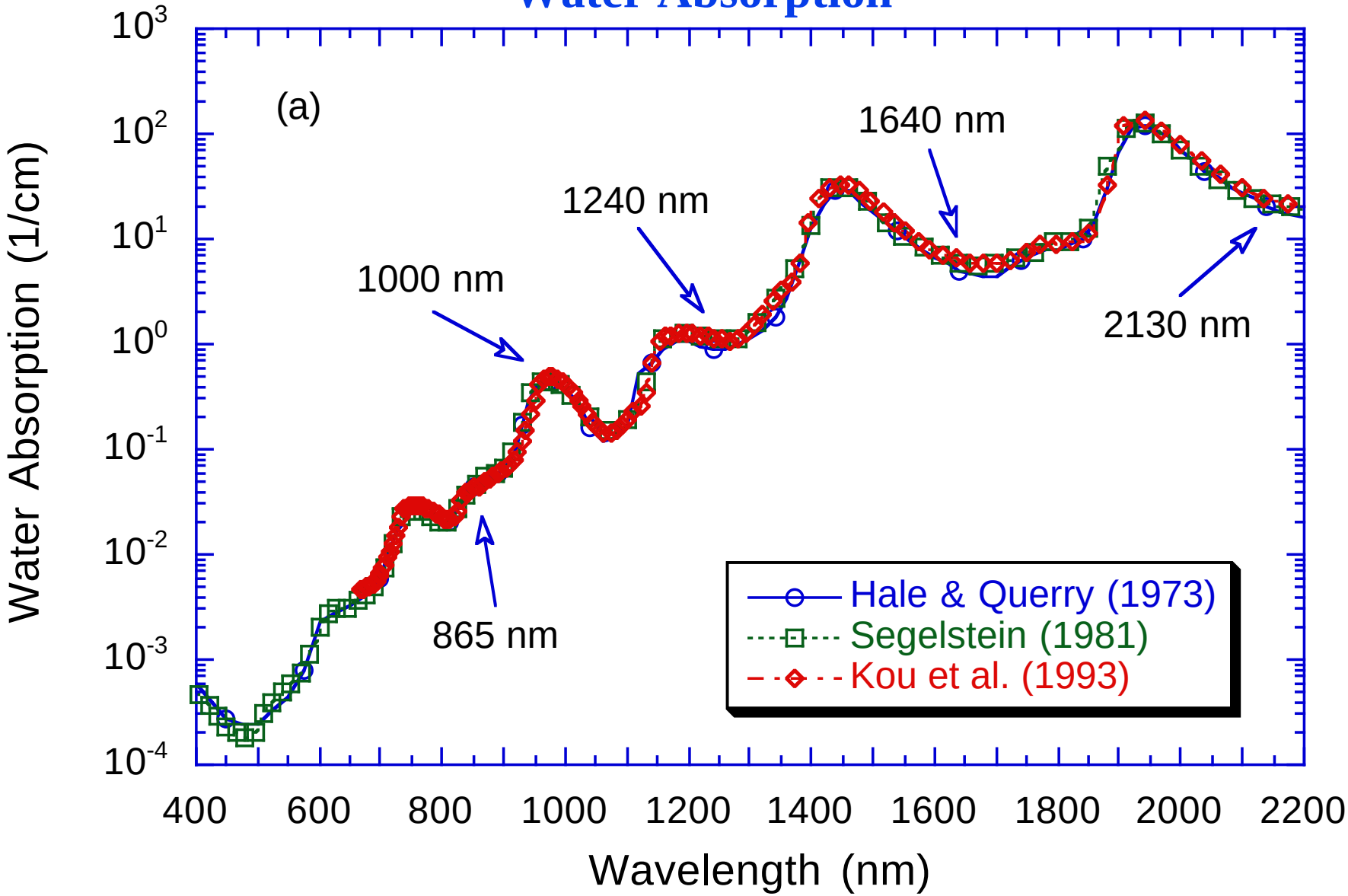

Black ocean at the SWIR bands: Absorption at the SWIR bands is at least an order larger than that at the 865 nm!

Aerosol Single-Scattering Epsilon (λ_0 = 1240 nm)

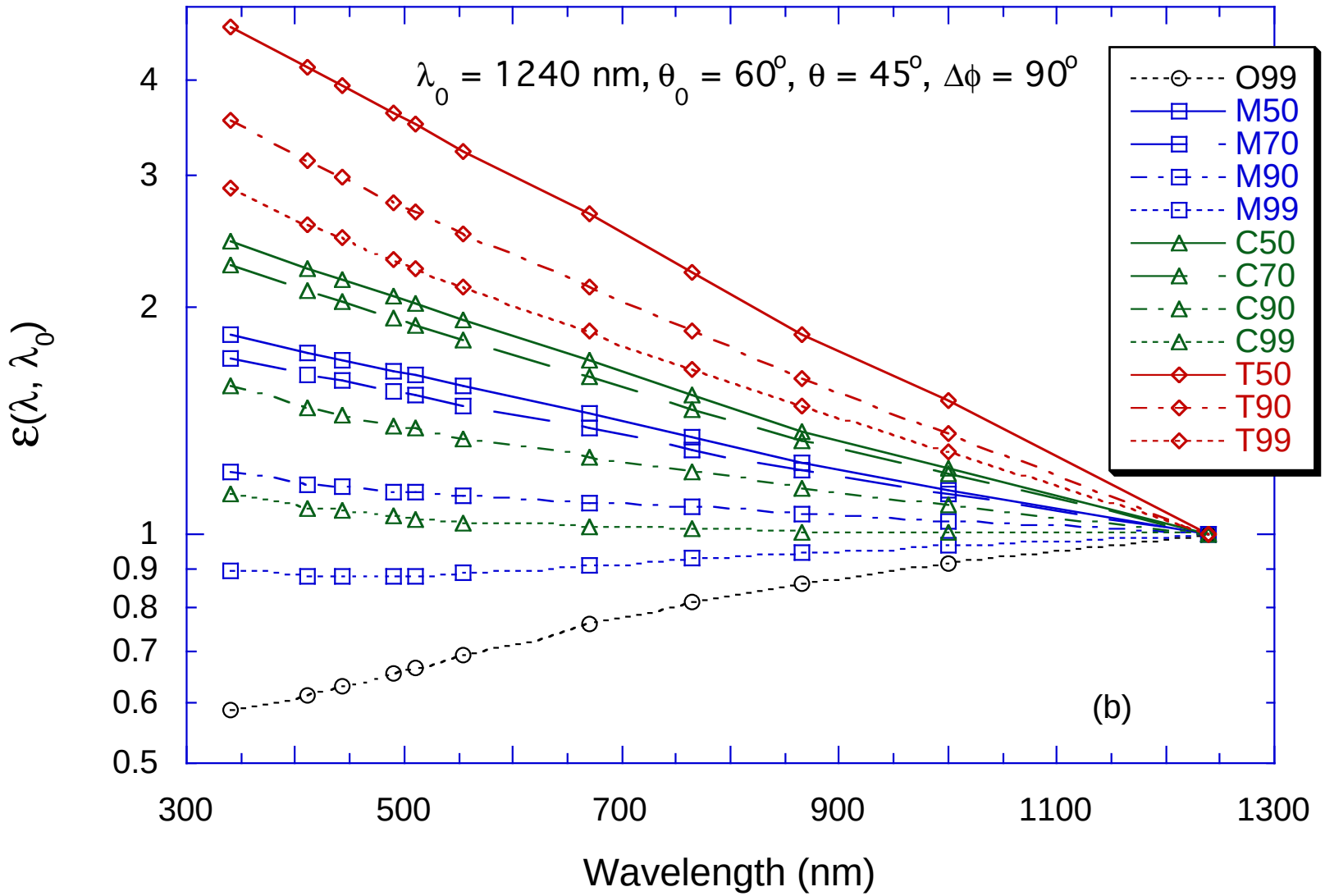

Aerosol Single-Scattering Epsilon (λ_0 = 1640 nm)

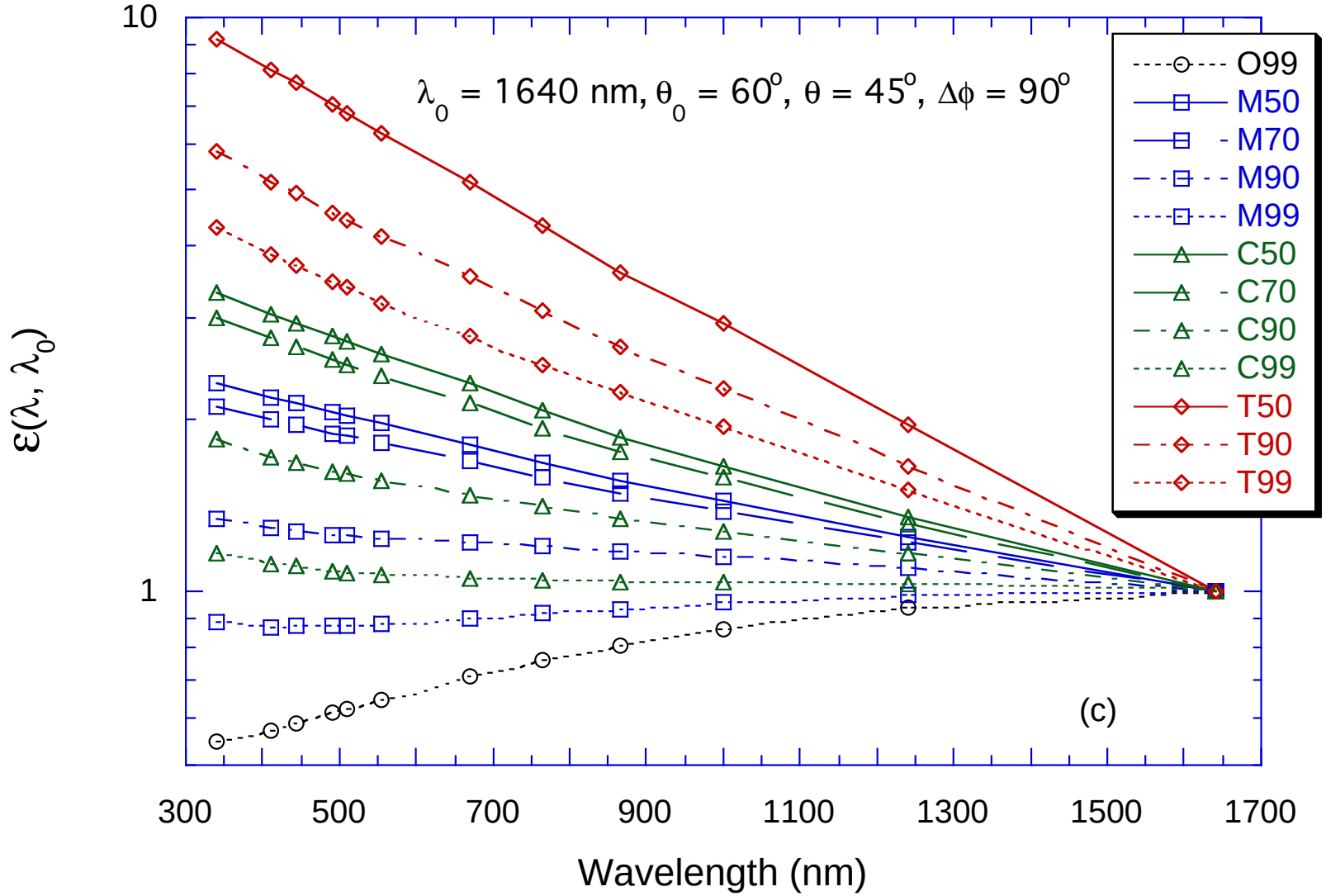

Aerosol Single-Scattering Epsilon (λ_0 = 2130 nm)

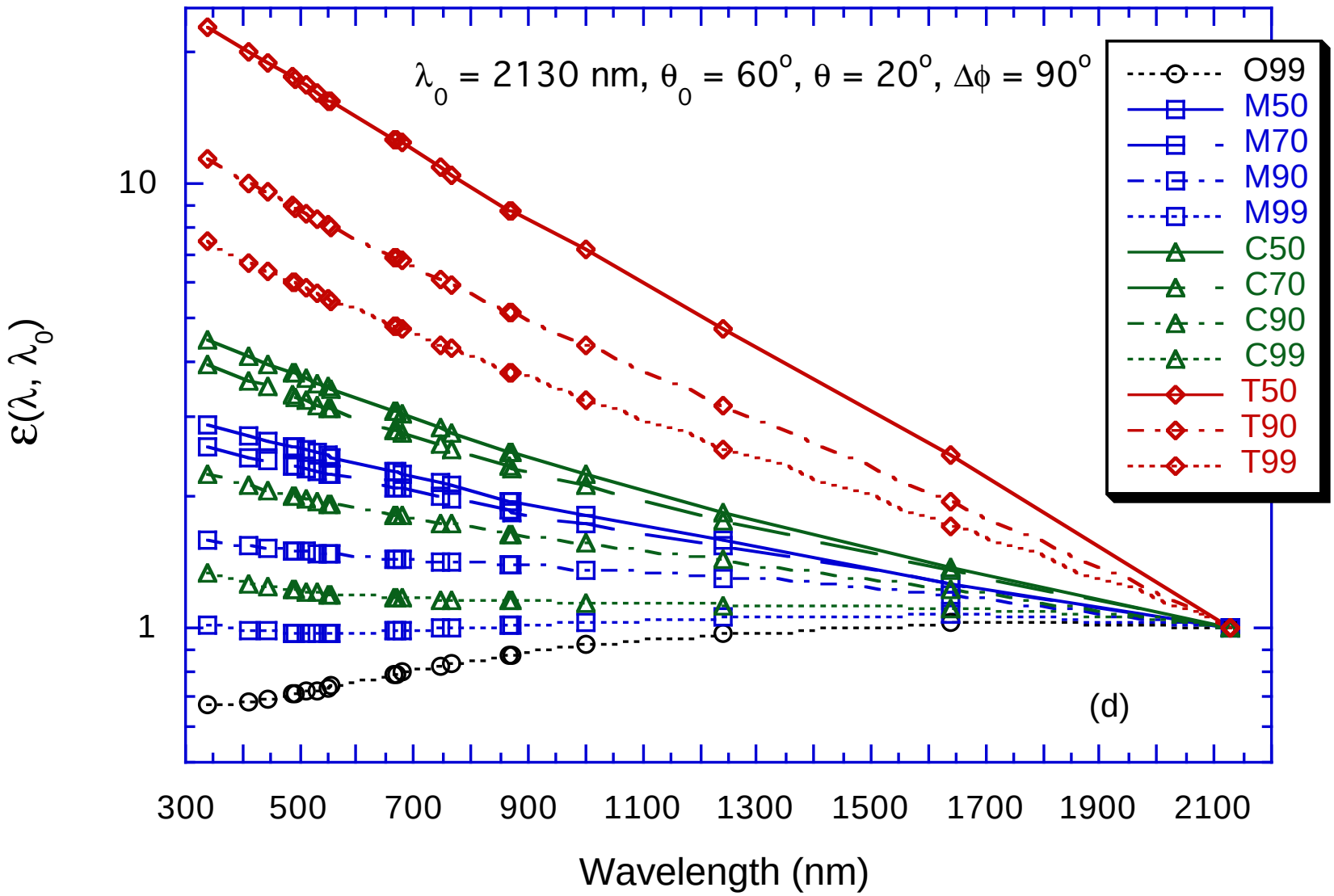

Data Processing (NOAA-MSL12) Using the SWIR Bands

Software Modifications:

- Atmospheric correction package has been significantly modified based on SeaDAS 4.6.
- Data structure and format of aerosol lookup tables and diffuse transmittance tables have been changed.
- With these changes, it is flexible now to run with different aerosol models (e.g., absorbing aerosols) and with various band combinations for atmospheric correction.

Lookup Tables Generation and Implementation:

- Rayleigh lookup tables for the SWIR bands (for all MODIS 16 bands).
- Aerosol optical property data (scattering phase function, single scattering albedo, extinction coefficients) for the SWIR bands (12 models).
- Aerosol radiance lookup tables (12 aerosol models) for the SWIR bands (for all MODIS 16 bands). Vector RTE (with polarization) were used for aerosol LUTs generation.

Data Processing:

- Regenerated MODIS L1B data including all SWIR band data (for SeaDAS).
- Developed cloud masking using the MODIS SWIR 1240 nm band.
- For MODIS Aqua, atmospheric correction can be operated using 1240/2130 nm bands, 1640/2130 nm bands.
- Current 16 bands: 412, 443, 469, 488, 531, 551, 555, 645, 667, 678, 748, 859, 869, 1240, 1640, and 2130 nm.

Vicarious calibration:

- SWIR and NIR-SWIR algorithms (data processing systems) have been vicariously calibrated to produce consistent ocean color products.

5.6. Examples from MODIS-Aqua measurements

Results from SWIR Atmospheric Correction for turbid ocean waters in US east coastal

MODIS-Aqua True Color Image

U.S. East Coastal

April 6, 2004

Ocean Spectra from Visible to NIR for Various Ocean Waters

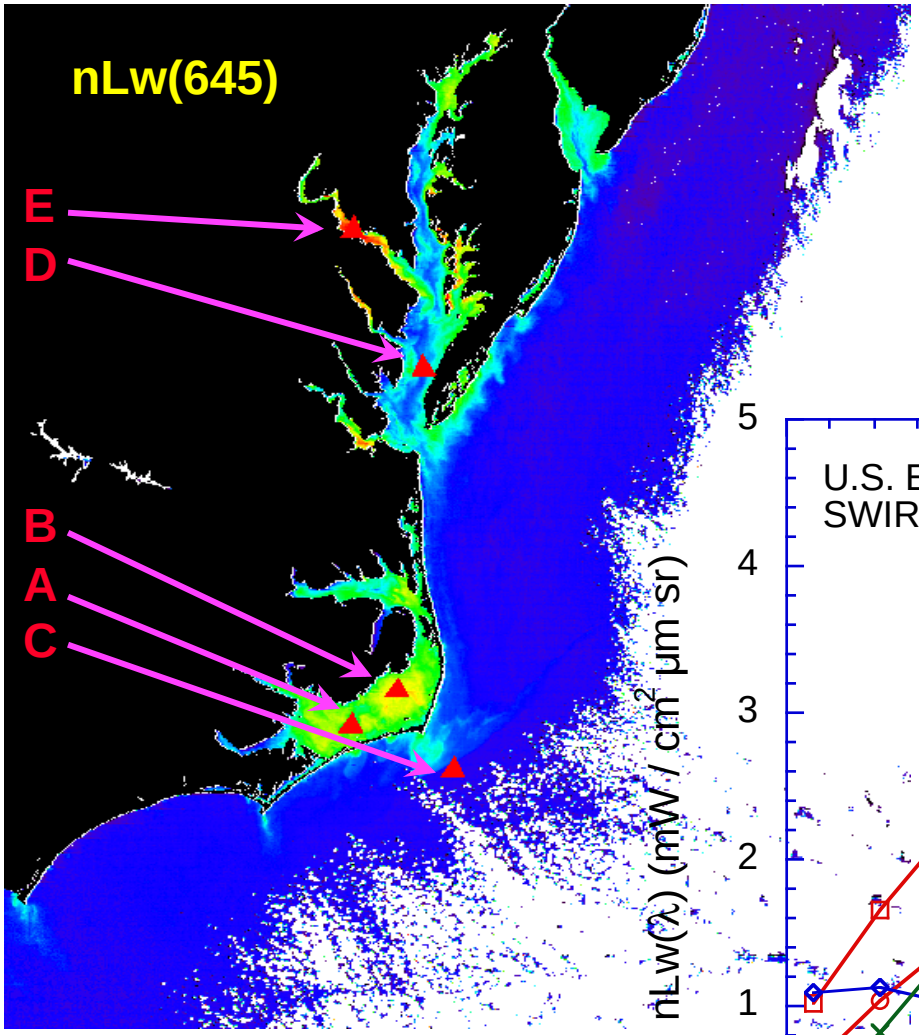

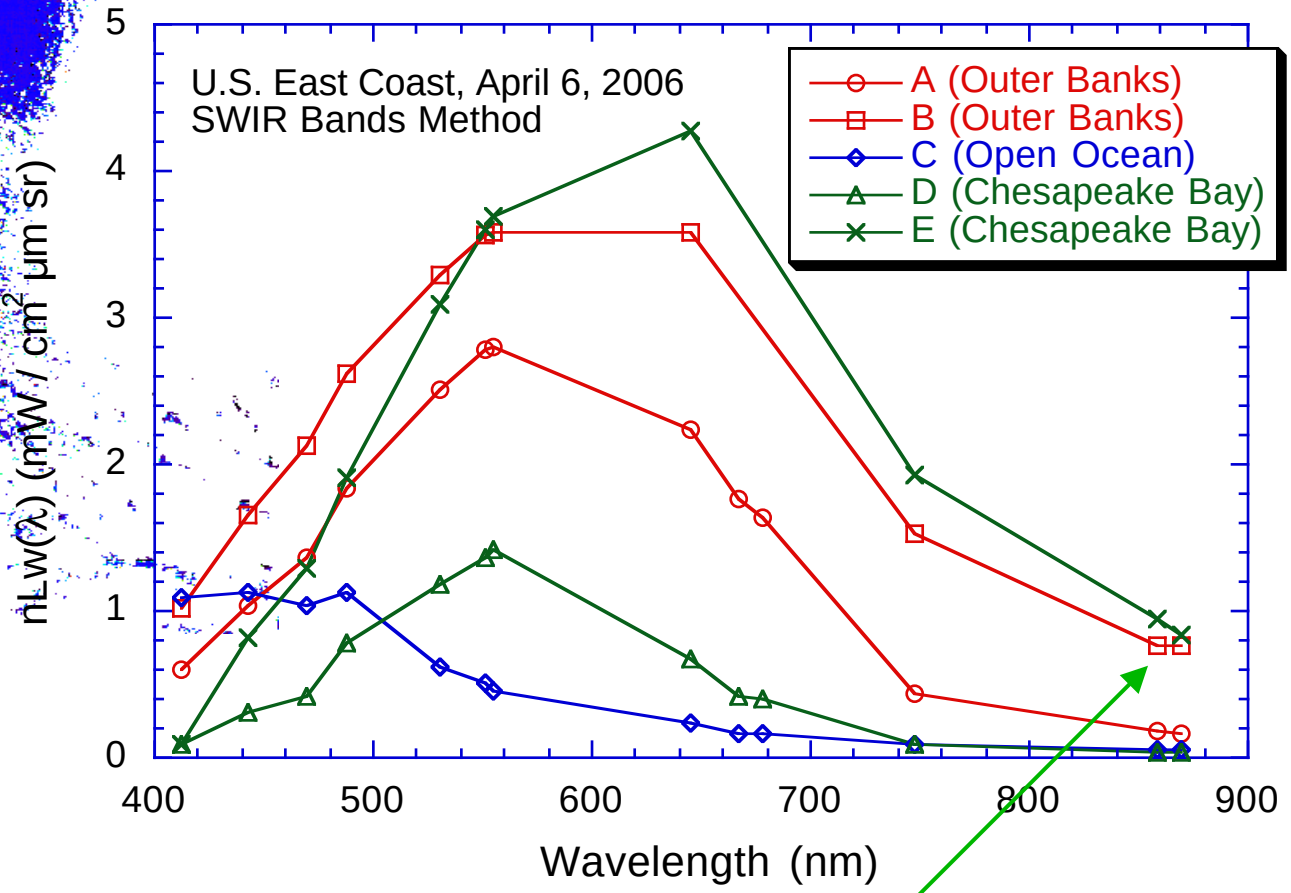

$\tau_a(869) \sim 0.3$

Comparisons of MODIS Ocean Color Products from NIR, SWIR, and NIR-SWIR Combined Methods

Example: U.S. East Coast

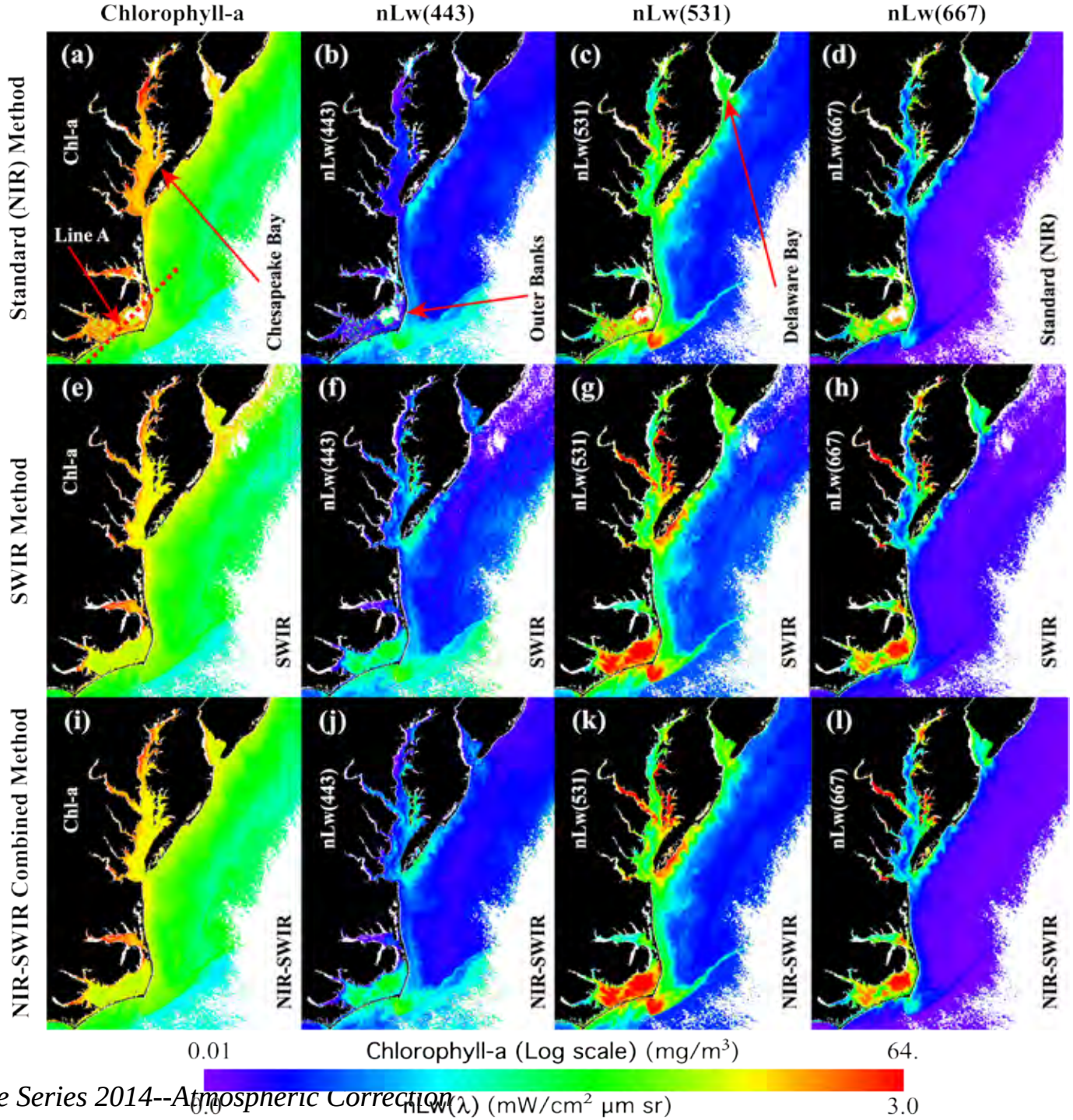

Wang, M. and W. Shi (2007), "The NIR-SWIR combined atmospheric correction approach for MODIS ocean color data processing," *Optics Express*, **15**, 15722-15733.

Results from MODIS-Aqua Measurements

(Chesapeake Bay)

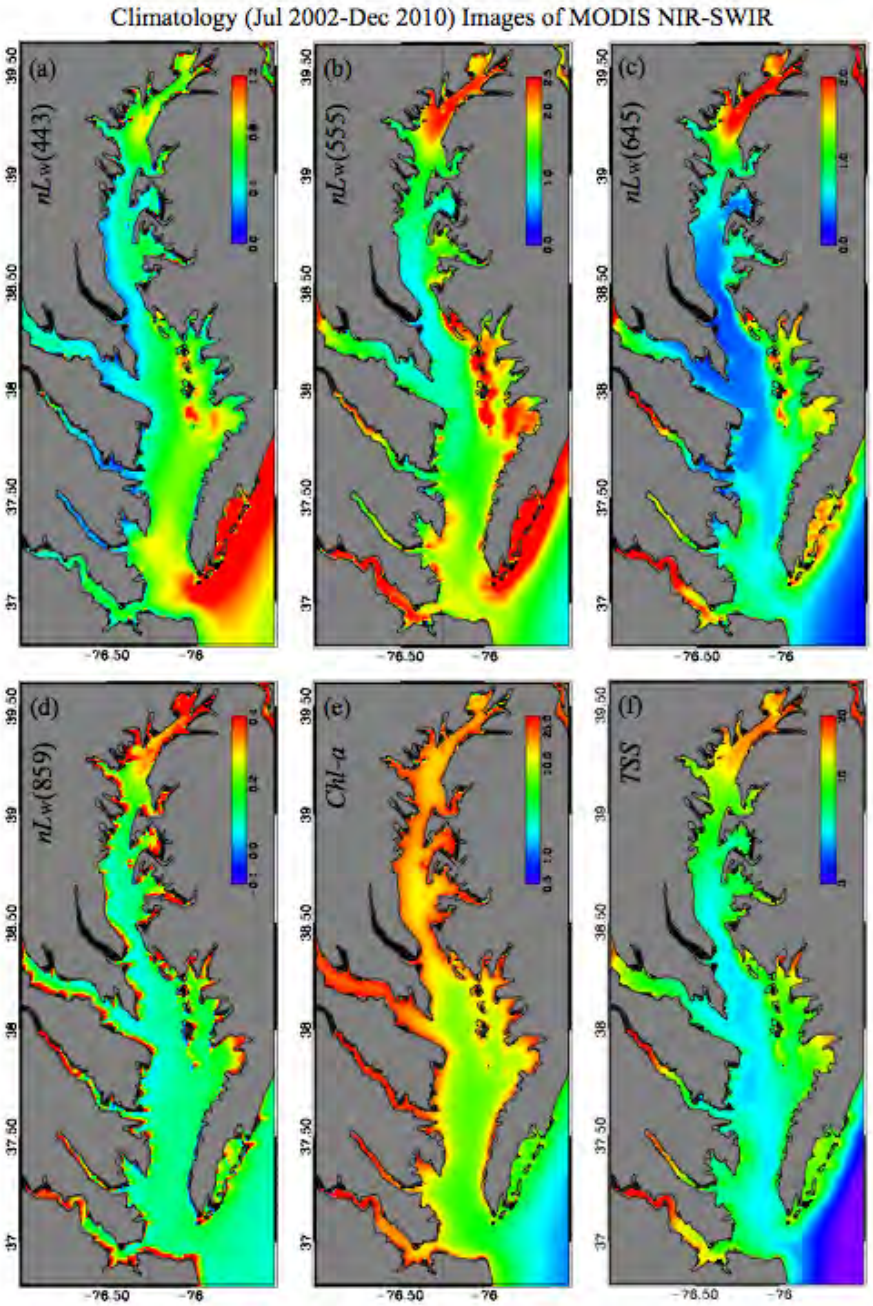

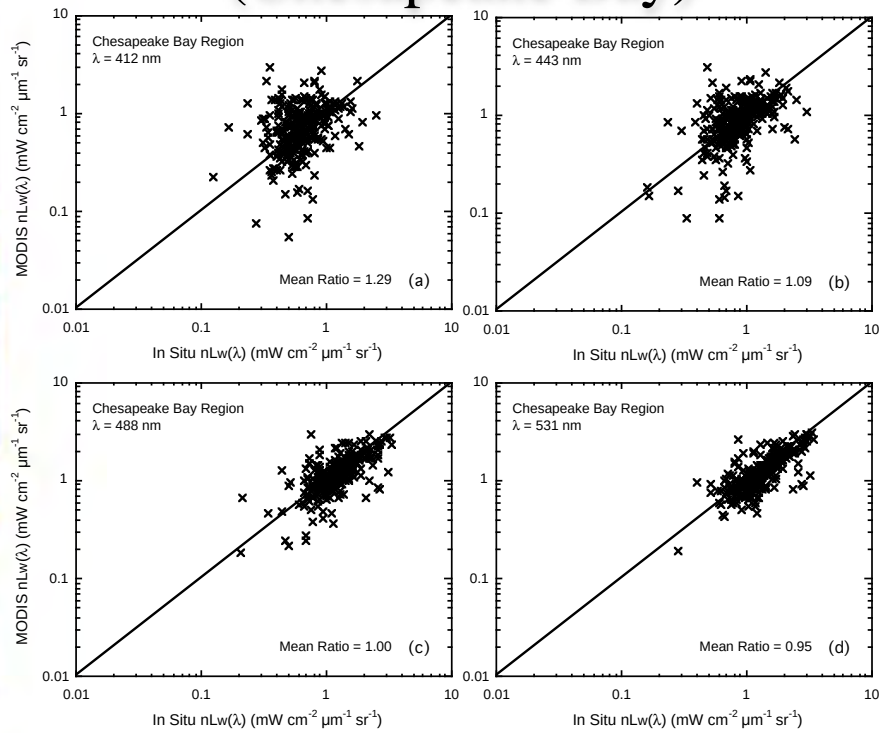

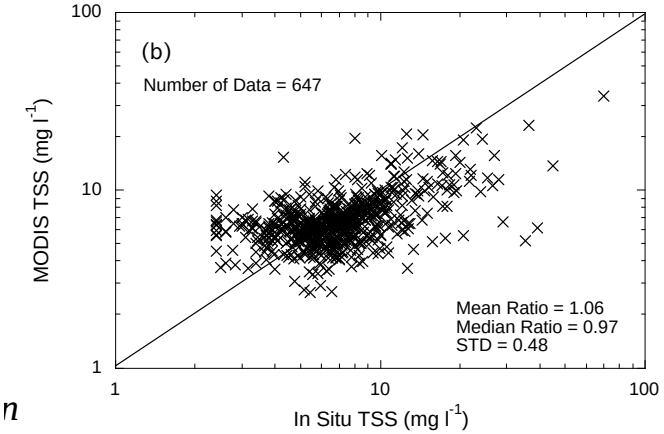

n

Results from MODIS-Aqua Measurements

(China East Coast)

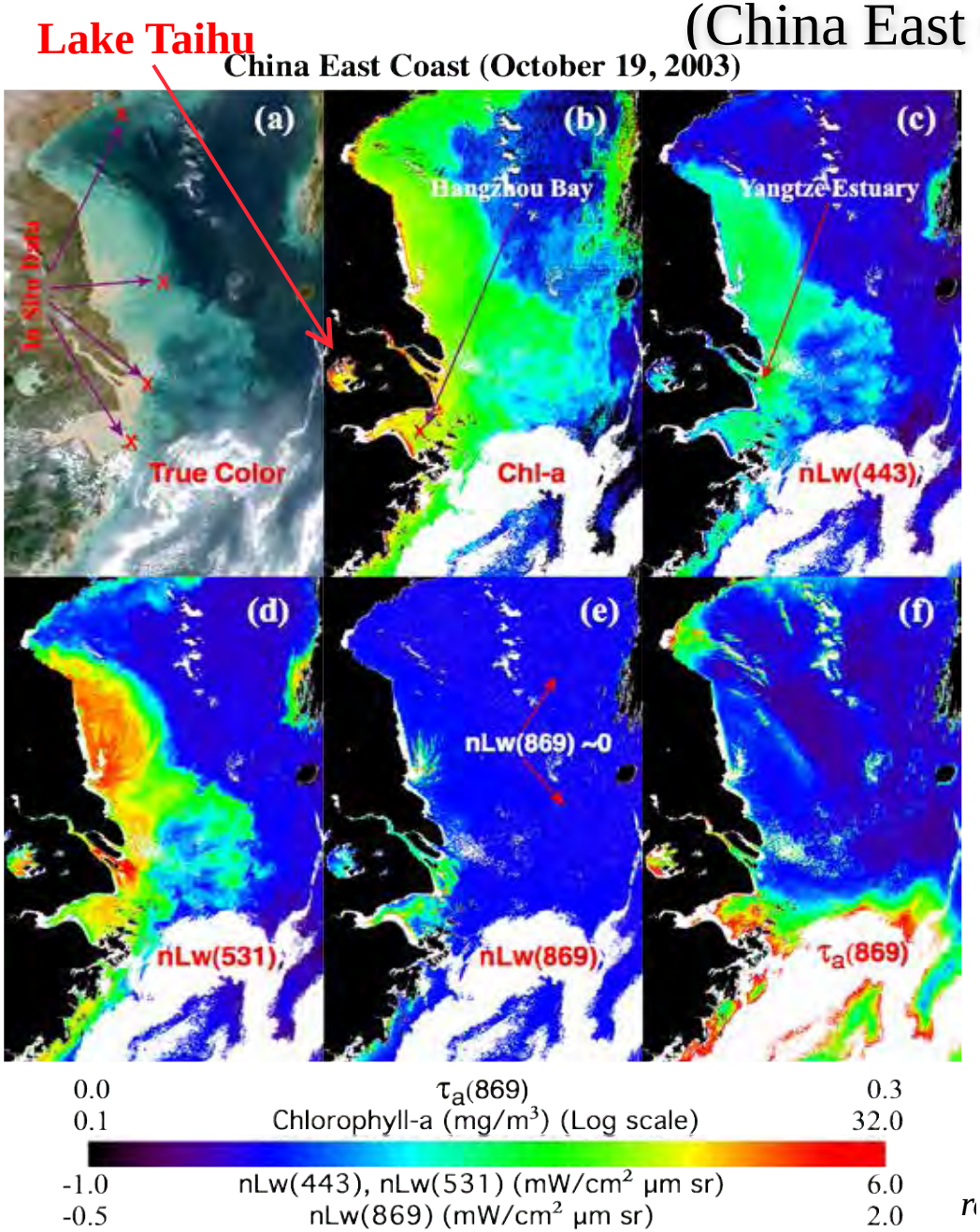

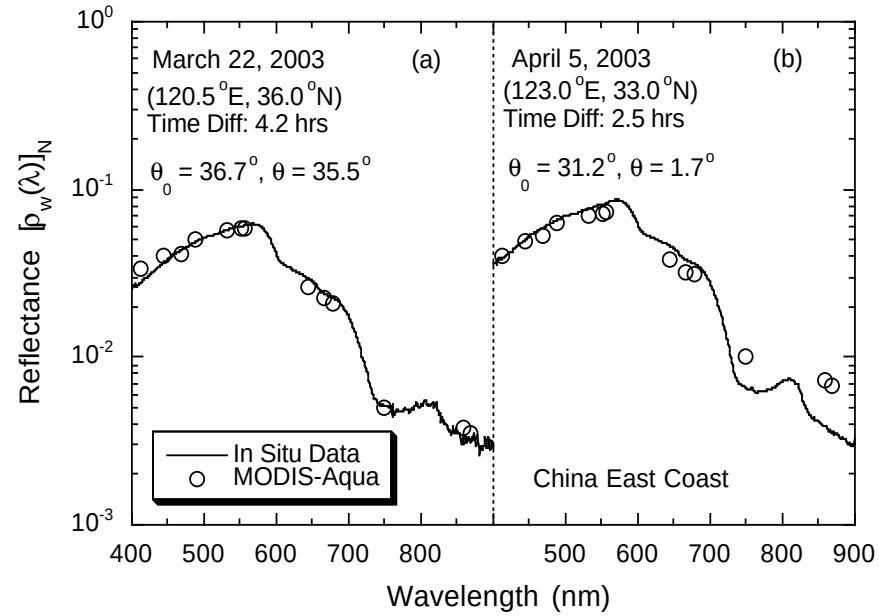

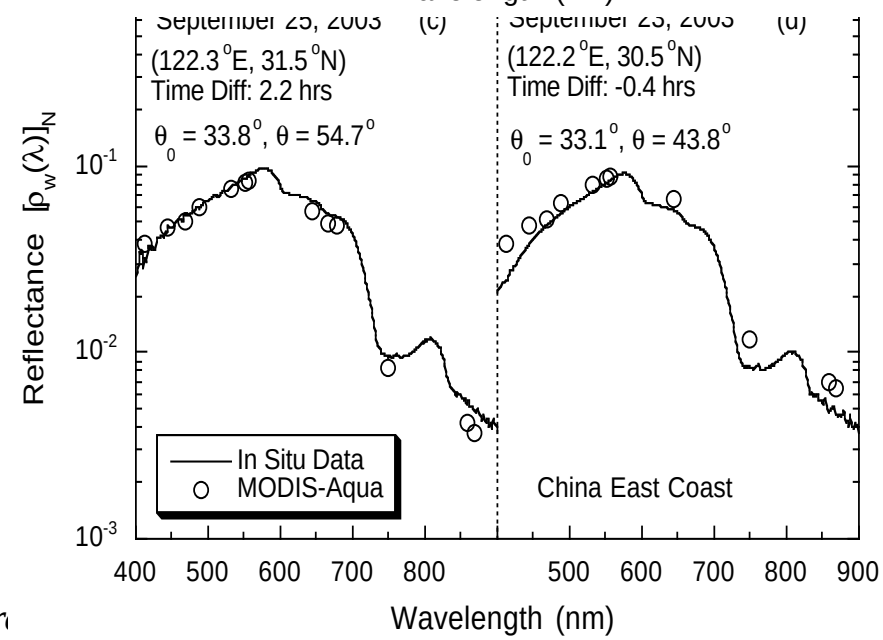

Validation Results (3)

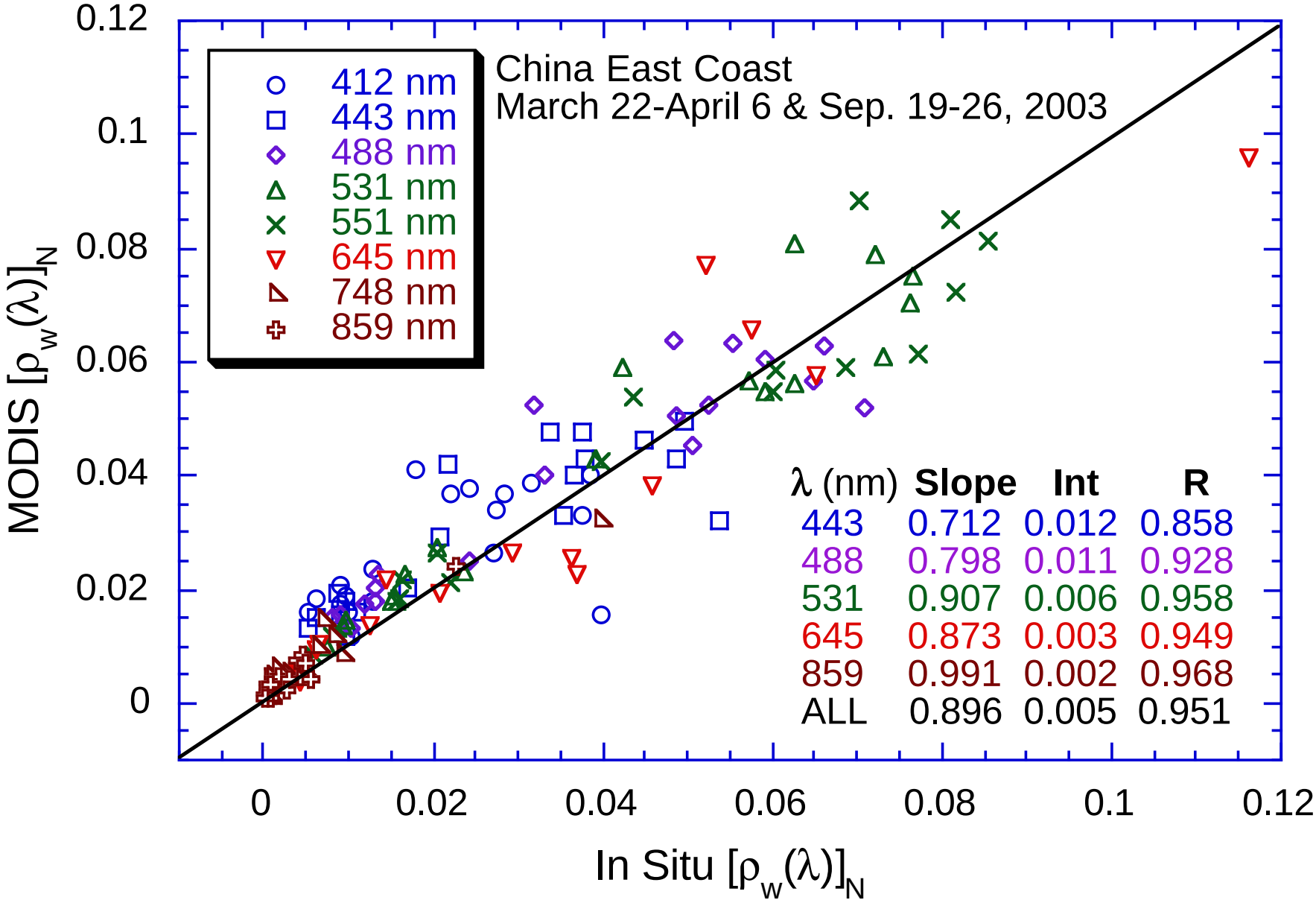

Water-leaving Radiance Spectra in Hangzhou Bay

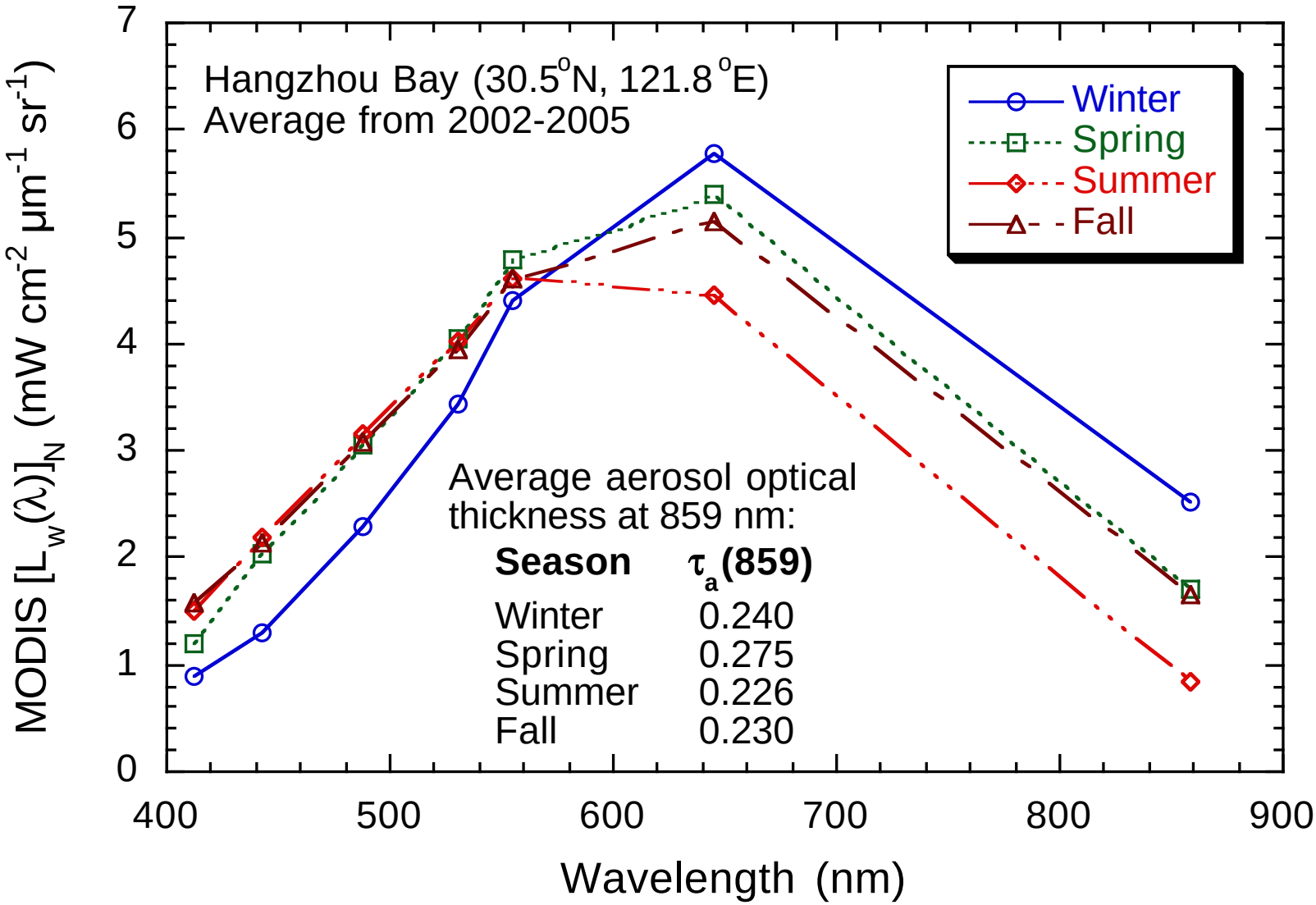

nLw(443)

Scale: 0.-3.0
(mW/cm^2 µm sr)

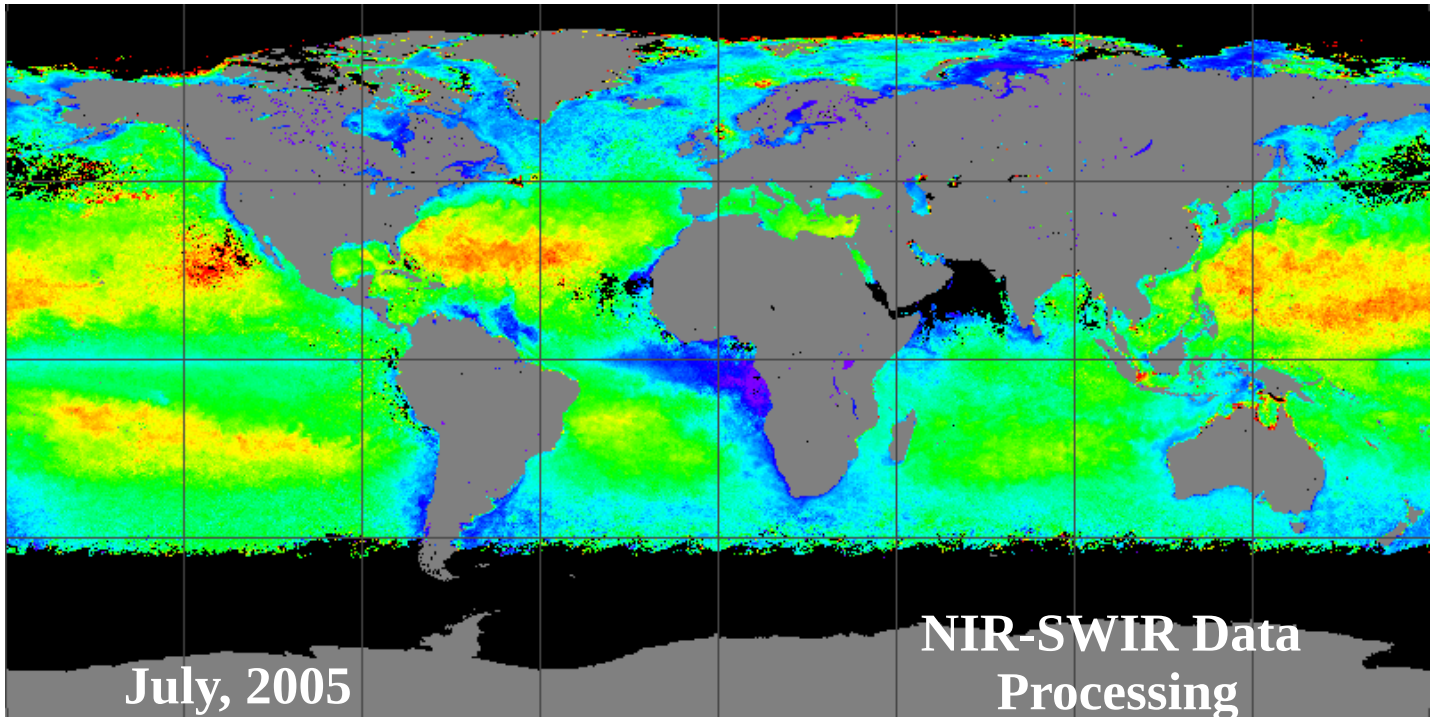

Chlorophyll-a

0.01-10 (mg/m^3)
(Log scale)

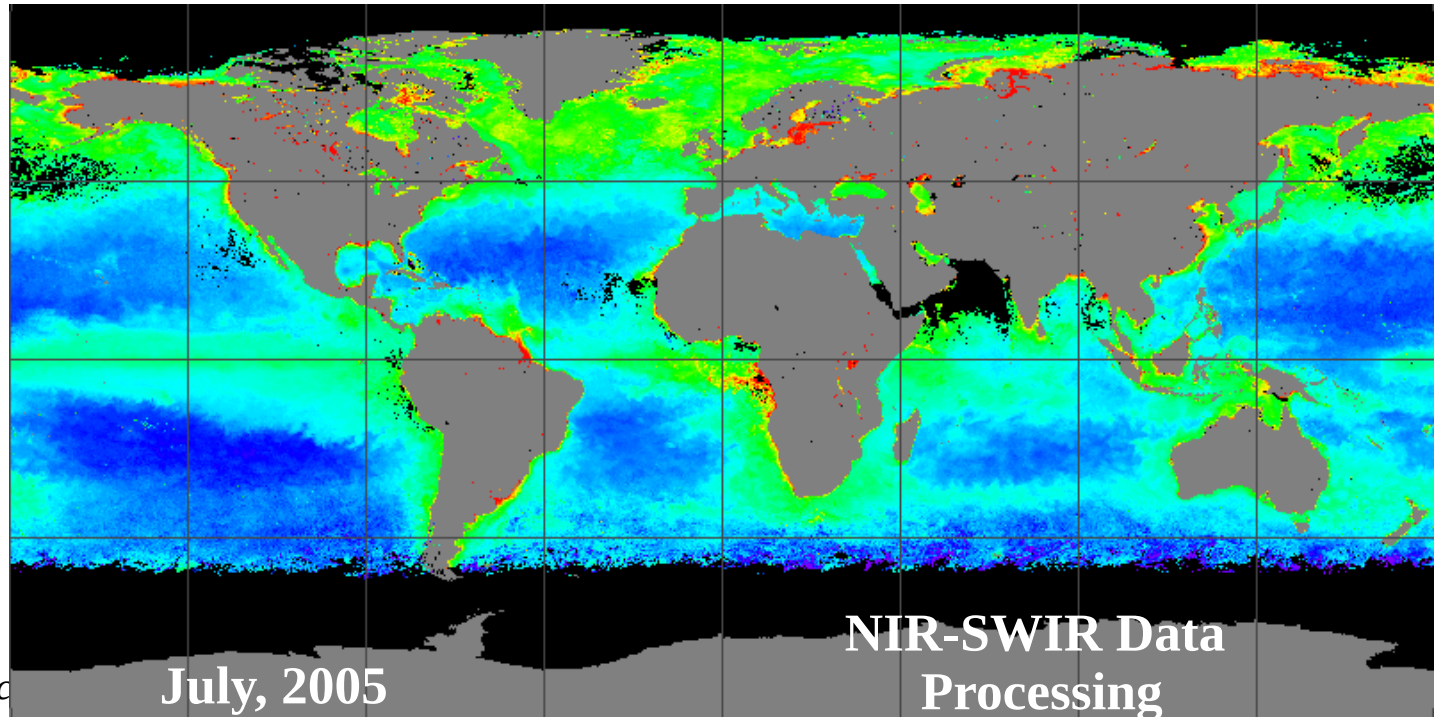

Wang, M., S. Son, and W. Shi (2009), "Evaluation of MODIS SWIR and NIR-SWIR atmospheric correction algorithms using SeaBASS data," *Remote Sens. Environ.*, **113**, 635-644.

The SWIR 1240 nm band is not black for extremely turbid waters in Hangzhou Bay

(Shi & Wang, 2009)

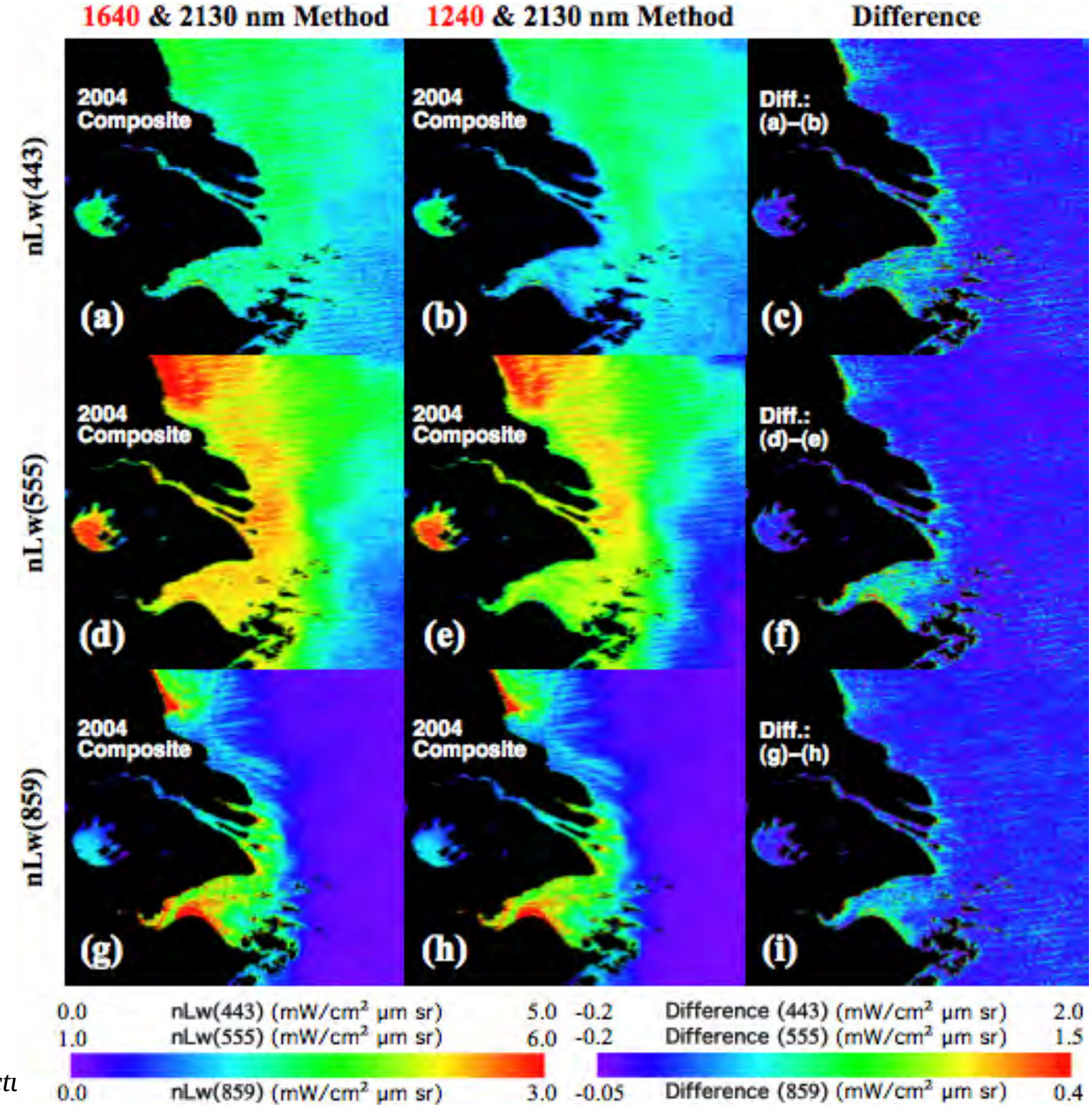

The SWIR 1240 nm band is not black for extremely turbid waters in La Plata Estuary

(Shi & Wang, 2009)

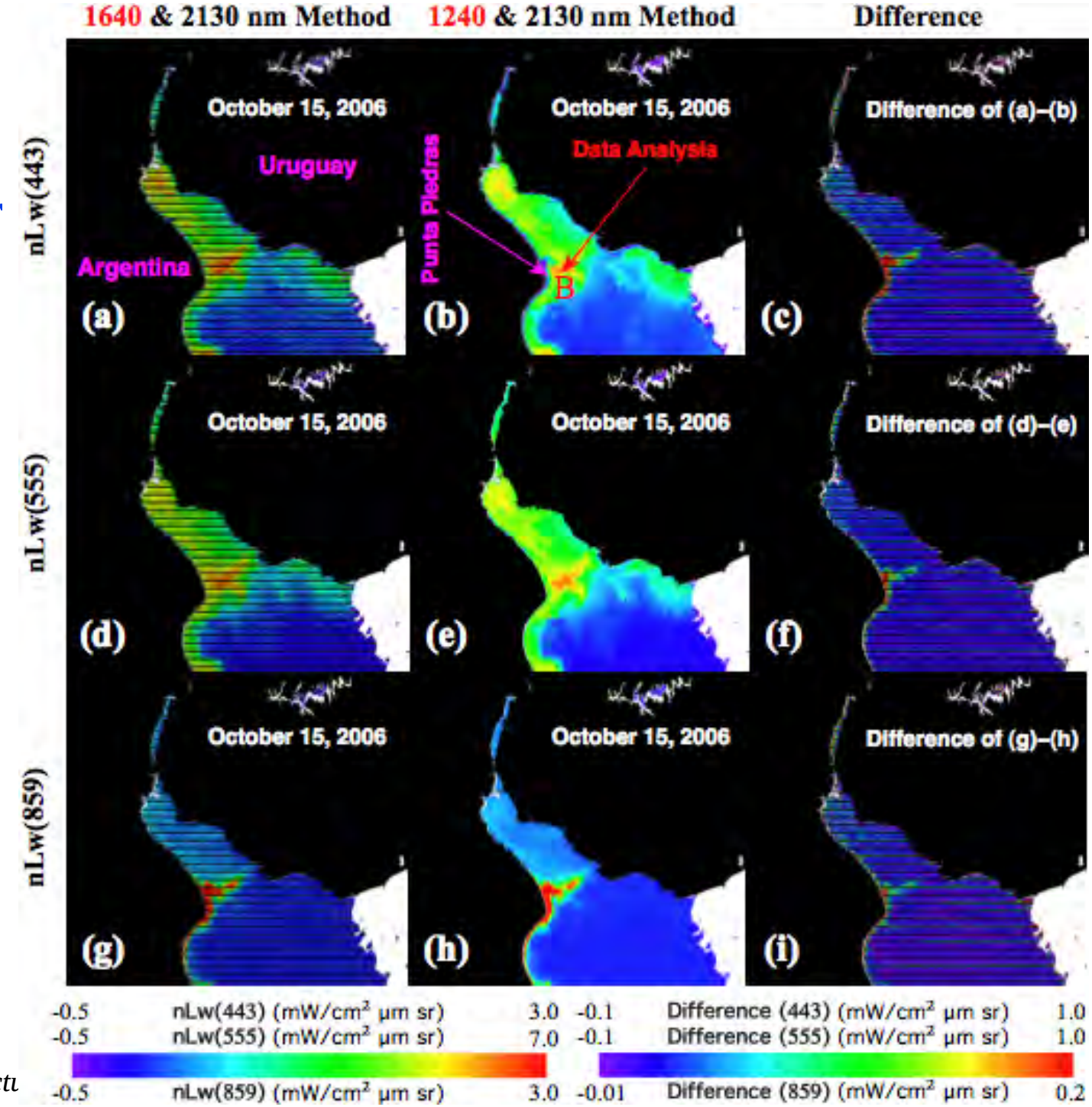

Menghua Wang, IOCCG Lectu

The SWIR-Derived Ocean Radiance Relationships (Shi & Wang, 2009)

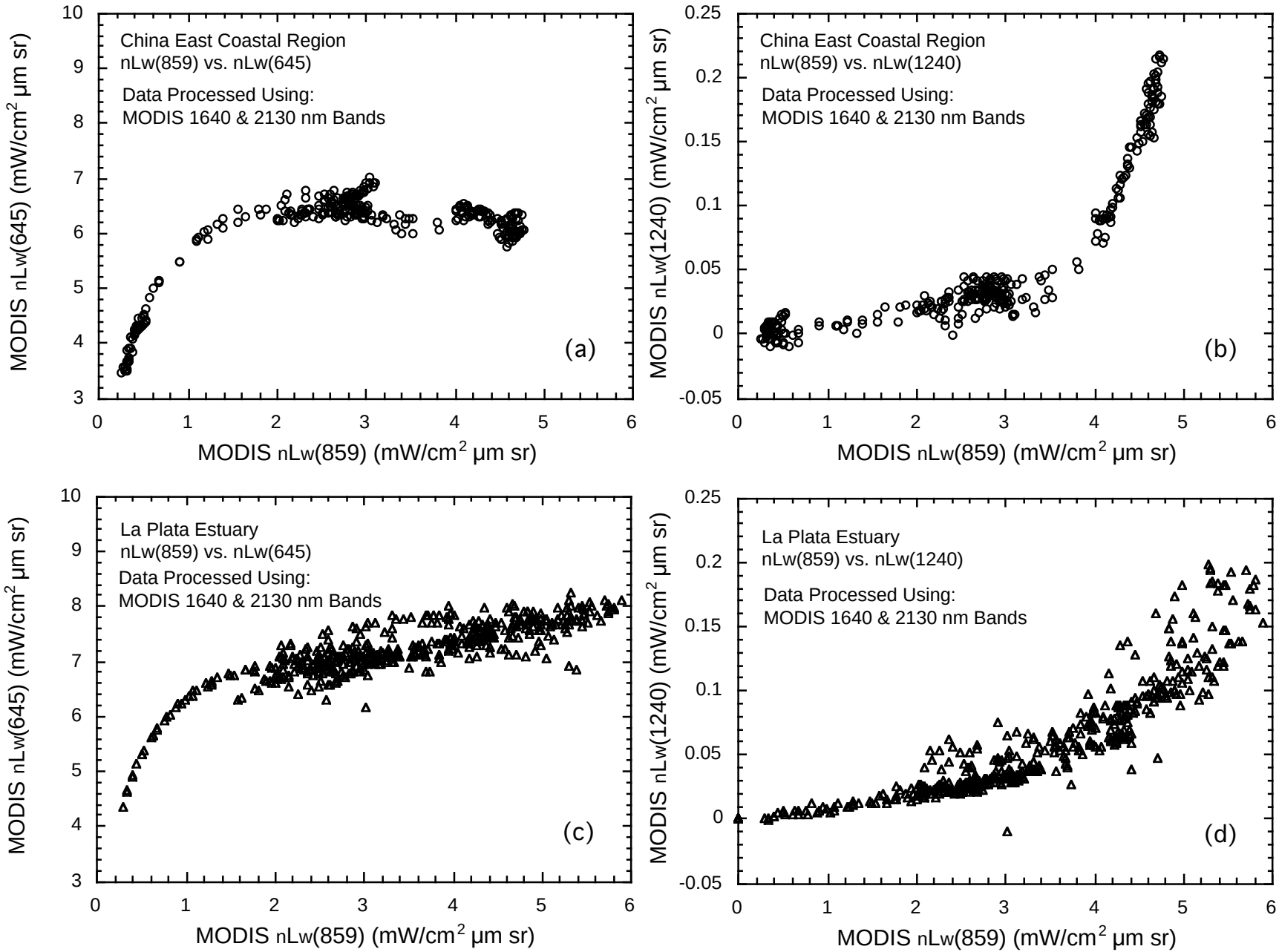

Blue-Green Algae (Microcystis) Bloom Crisis in Lake Taihu (Spring 2007)

Results from Inland Lake Taihu

Using the **SWIR** algorithm, we have derived the water optical properties over the Lake Taihu using the **MODIS-Aqua** measurements during the spring of 2007 for monitoring a **massive blue-green** algae bloom, which was a major natural disaster affecting several millions residents in nearby Wuxi city.

Wang, M. and W. Shi (2008), "Satellite observed algae blooms in China's Lake Taihu", *Eos, Transaction, American Geophysical Union*, **89**, p201-202, May 27.

Wang, M., W. Shi, and J. Tang (2011), "Water property monitoring and assessment for China's inland Lake Taihu from MODIS-Aqua measurements", *Remote Sens. Environ.*, **115**, 841-854.

- The work was featured in the NASA 2008 Sensing Our Planet (http://nasadaacs.eos.nasa.gov/articles/2008/2008_algae.html)

Acknowledgements

In situ data from Lake Taihu from **J. Tang** and **Y. Zhang**.

Geo-location of Lake Taihu

Extremely Turbid Waters

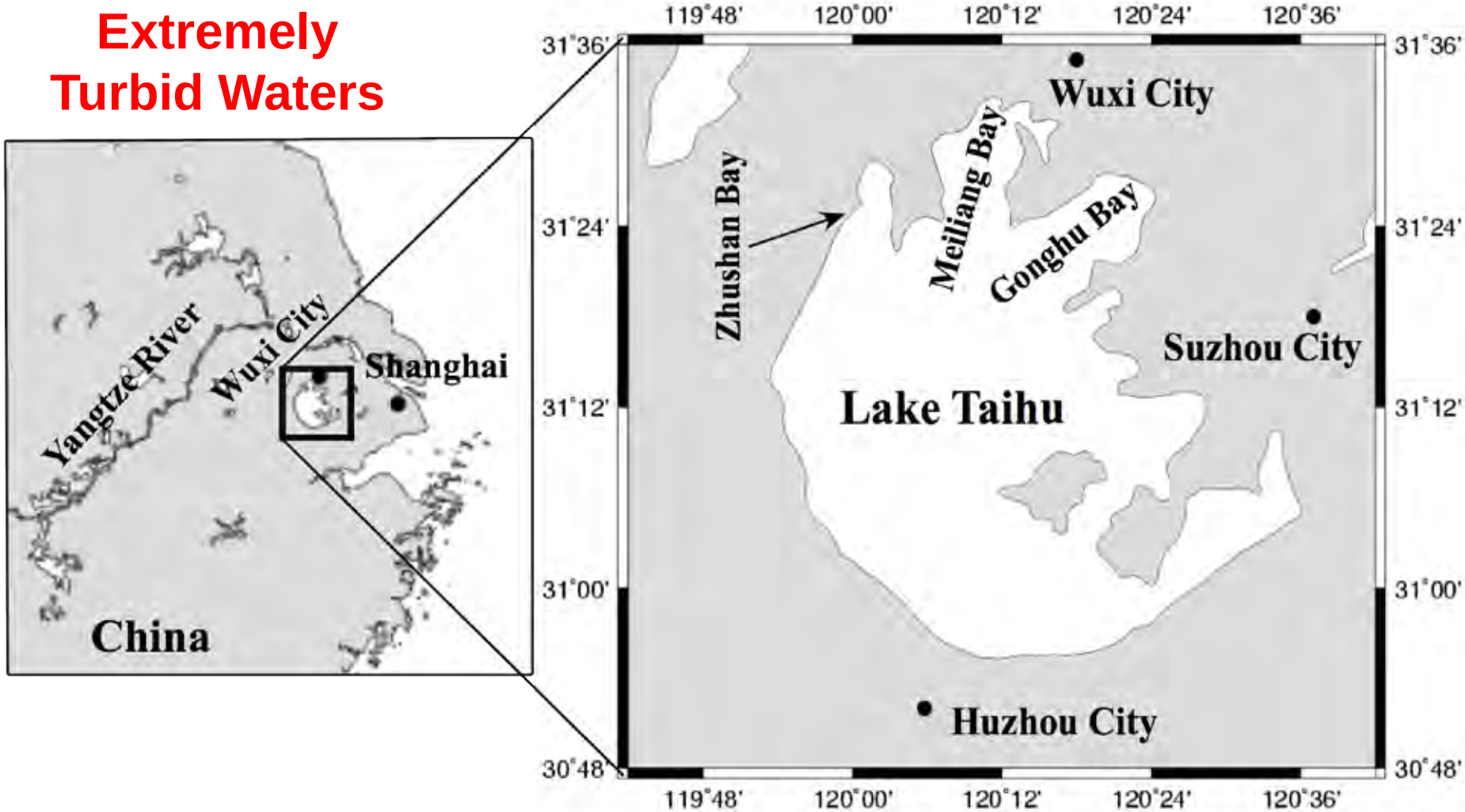

- ✓ The third largest fresh inland lake in China (~2,250 km^2).
- ✓ Located in one of the world's most urbanized and heavily populated areas.
- ✓ Provide water resource for several million residents in nearby Wuxi city.

Methodology (1)

- The SWIR atmospheric correction algorithm (Wang, 2007; Wang & Shi, 2005) is used for the water property data processing.
- Since MODIS 1240 nm band is not always black for the entire Lake Taihu, we have developed three-step method in the data processing for each MODIS-Aqua data file:
  - ✓ First, regions for the black of 1240 nm band are determined using the SWIR data processing.
  - ✓ Second, a dominant aerosol model from the region with black of 1240 nm band is obtained, and
  - ✓ Finally, with the derived aerosol model, the SWIR atmospheric correction algorithm is run using only 2130 nm band (with fixed aerosol model).
- The Lake Taihu water property data are then derived.

Wang, M., W. Shi, J. Tang (2011), "Water property monitoring and assessment for China's inland Lake Taihu from MODIS-Aqua measurement," *Remote Sens. Environ.*, **115**, 841-854.

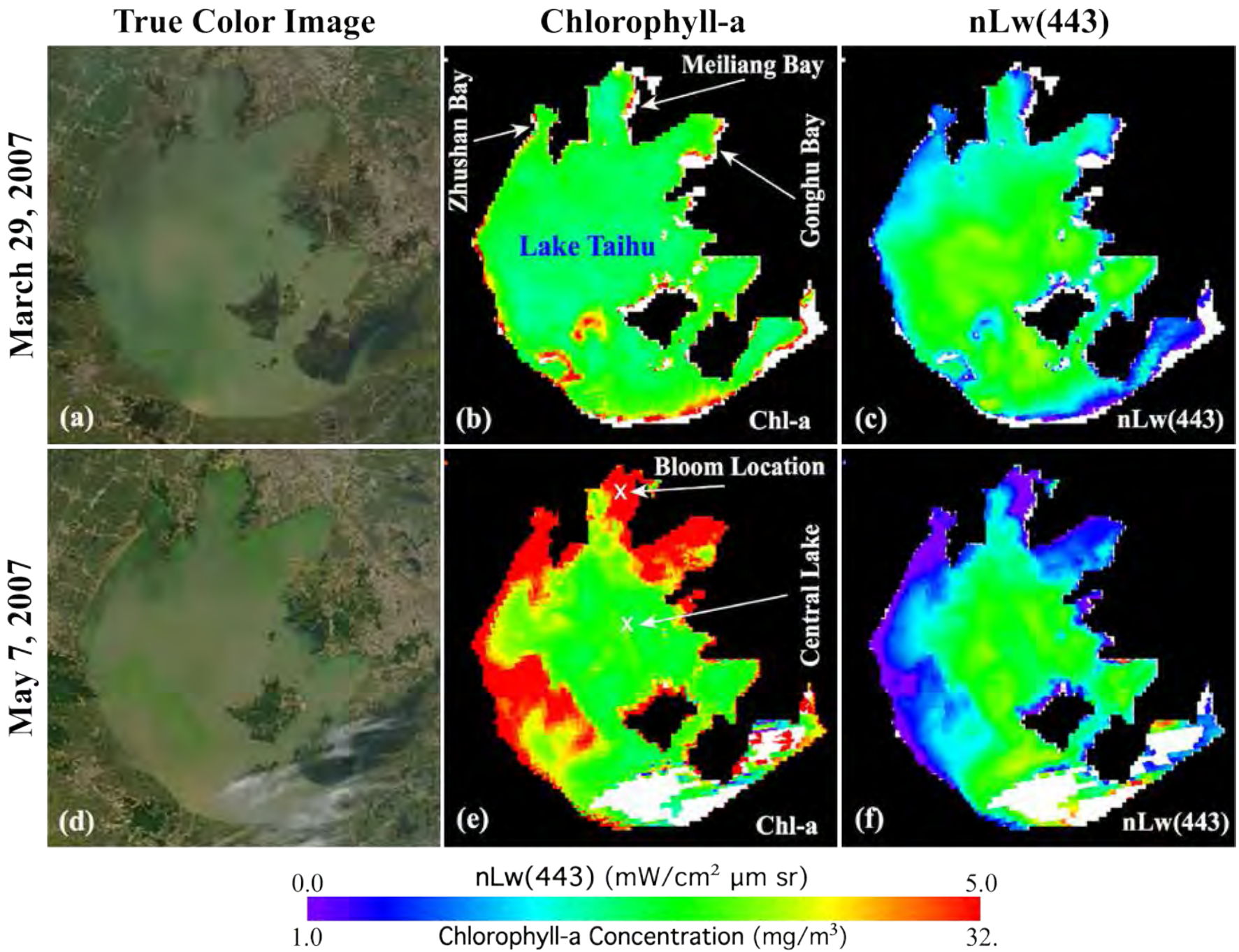

(*Wang and Shi*, 2008)

Time Series of Chlorophyll-a (index) and *nLw*(443) at Wuxi Station (bloom) and Central Lake (non-bloom)

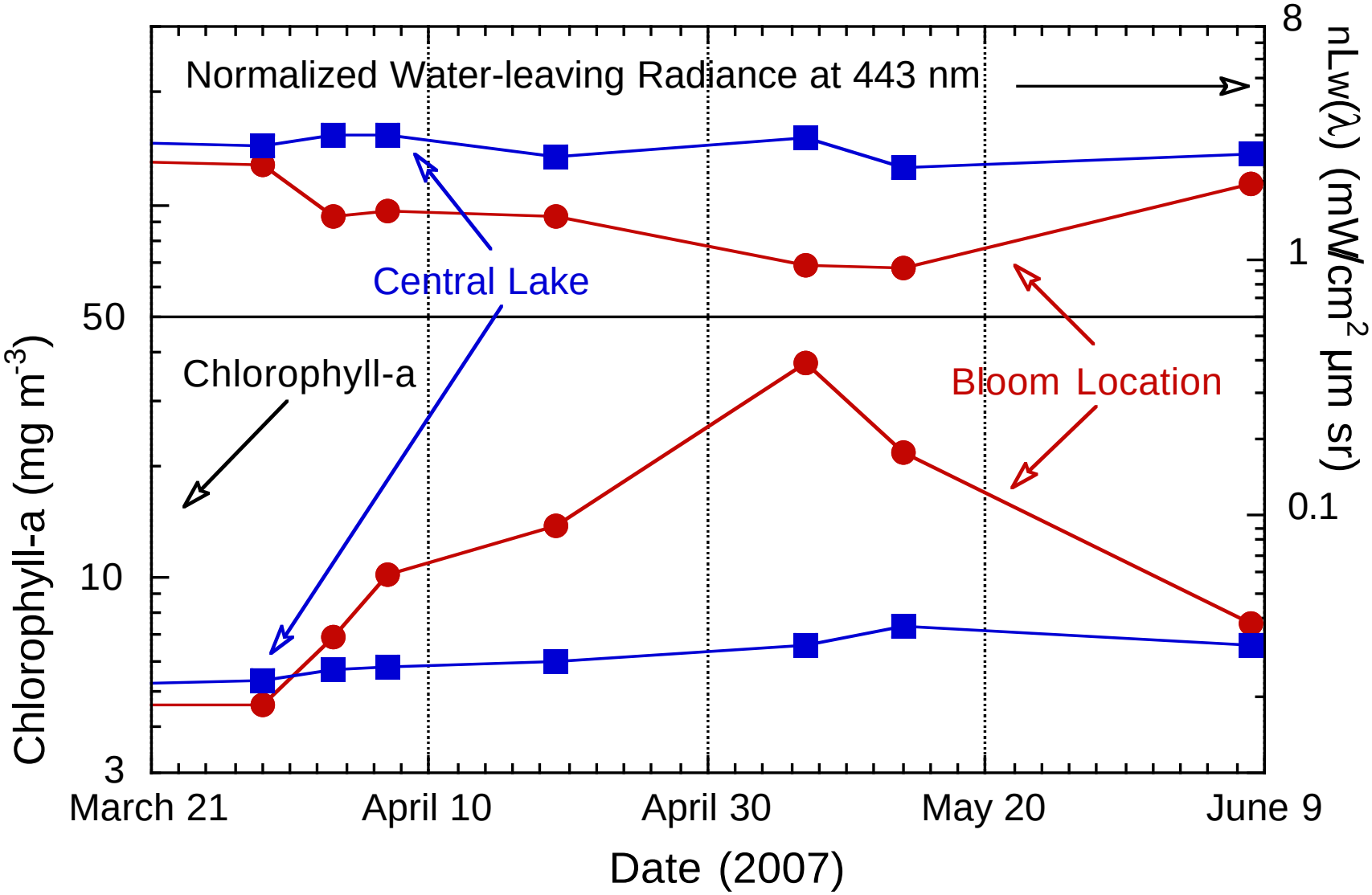

In Situ Data

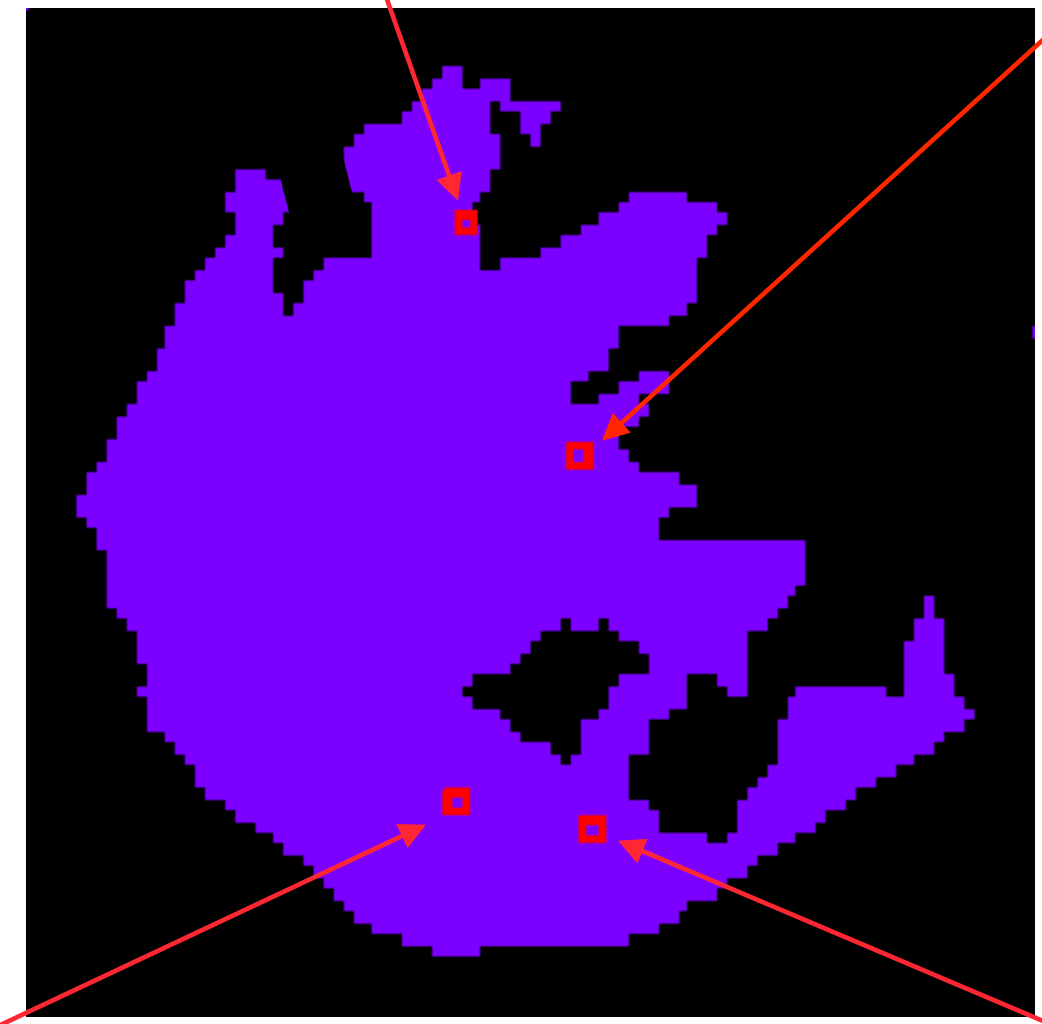

Validation Results for MODIS-derived Water-leaving Radiance Spectra

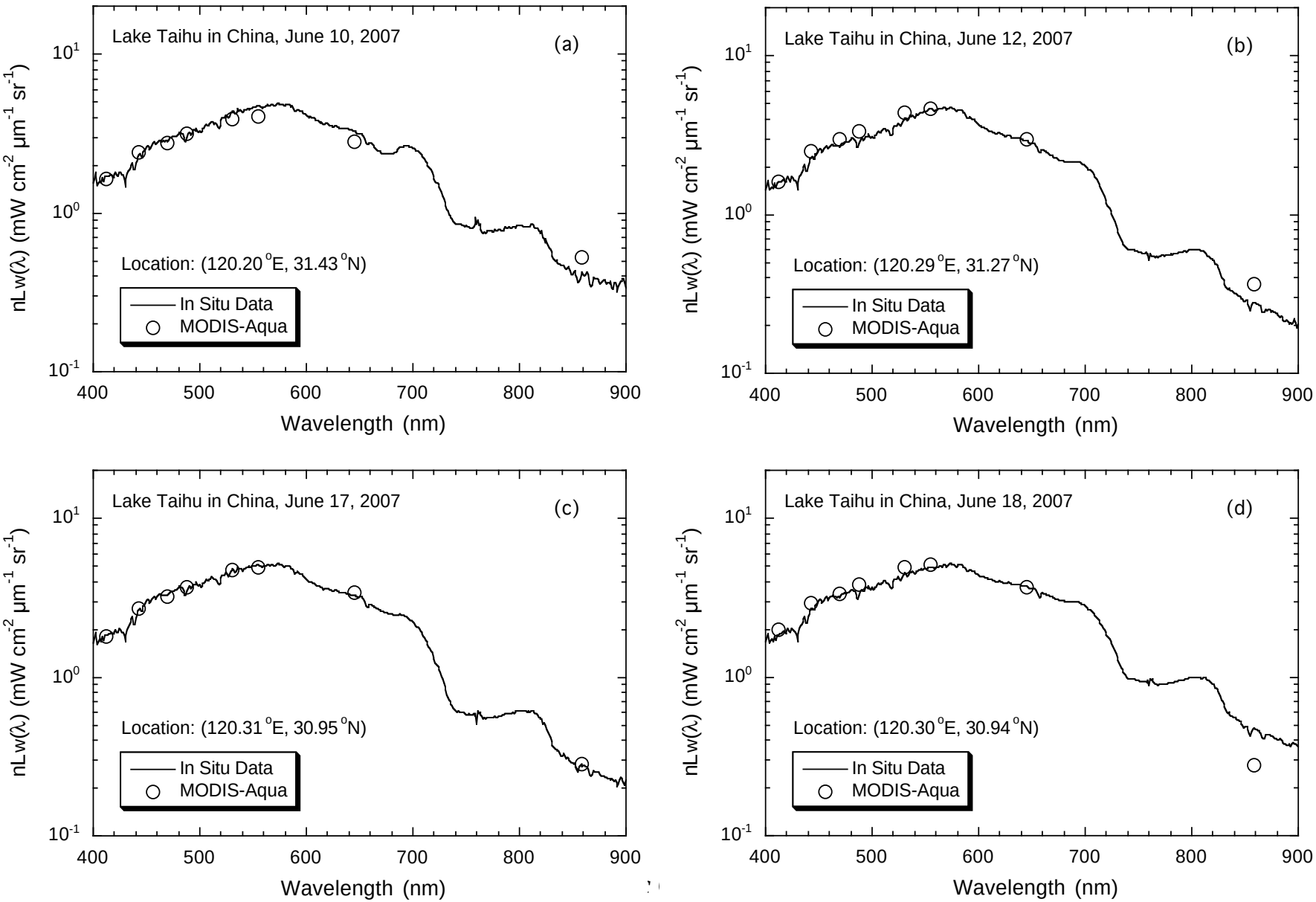

Methodology (2)

- Black pixel assumption at the SWIR 1640 and 2130 nm is generally valid for Lake Taihu.
- The SWIR atmospheric correction algorithm using bands 1640 and 2130 nm (Wang, 2007) can be used for the water property data processing.
- However, for MODIS-Aqua, four out of ten detectors for the SWIR 1640 nm band are inoperable (dysfunctional).
- We focus on deriving seasonal results for the lake using the SWIR 1640 and 2130 nm atmospheric correction algorithm.
- More in situ data (five seasonal cruises in 2006-2007 in the lake) are also available to us now.

Validation Results for MODIS-derived Water-leaving Radiance Spectra

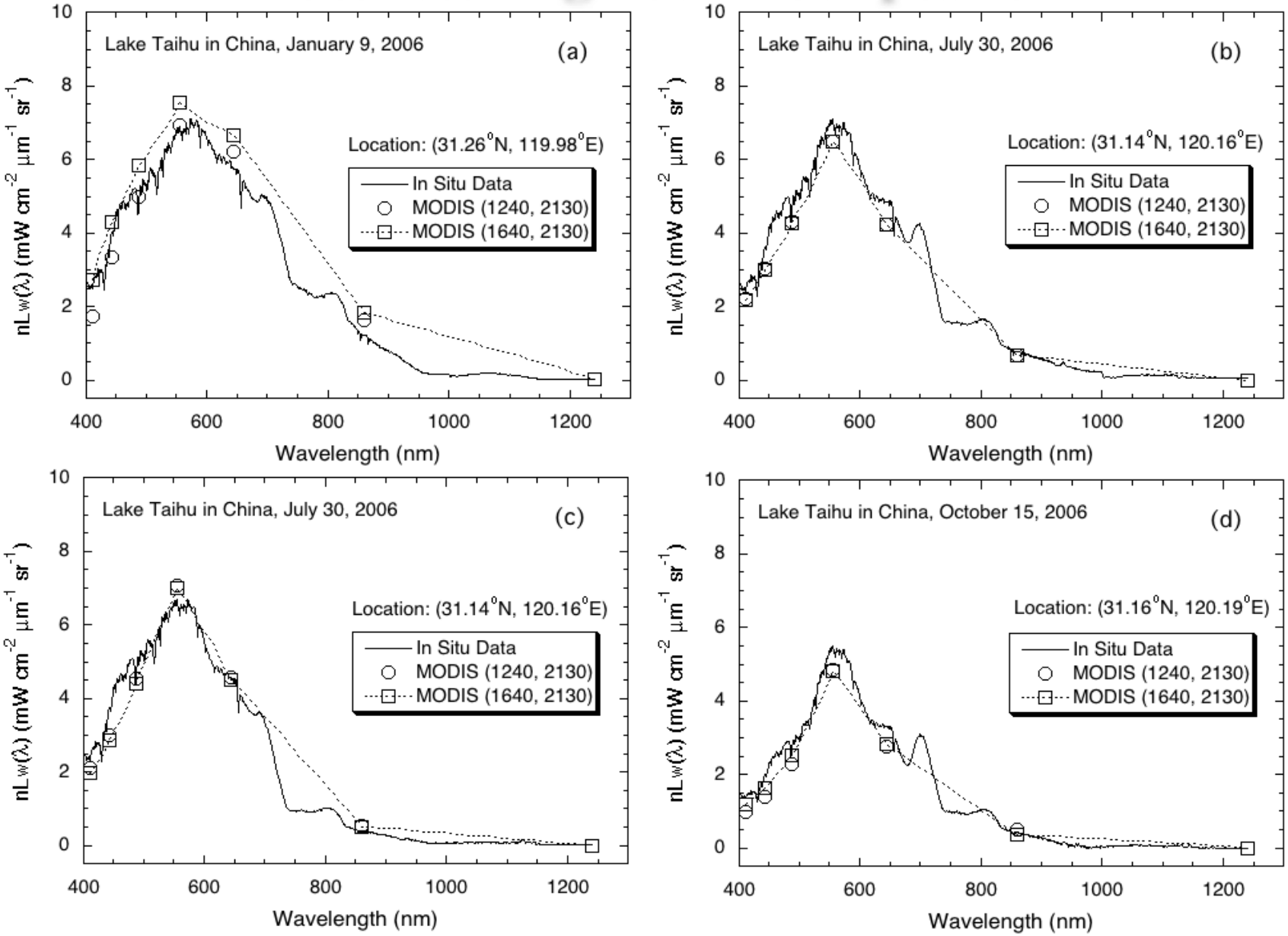

Validation Results in Lake Taihu (Method 2)

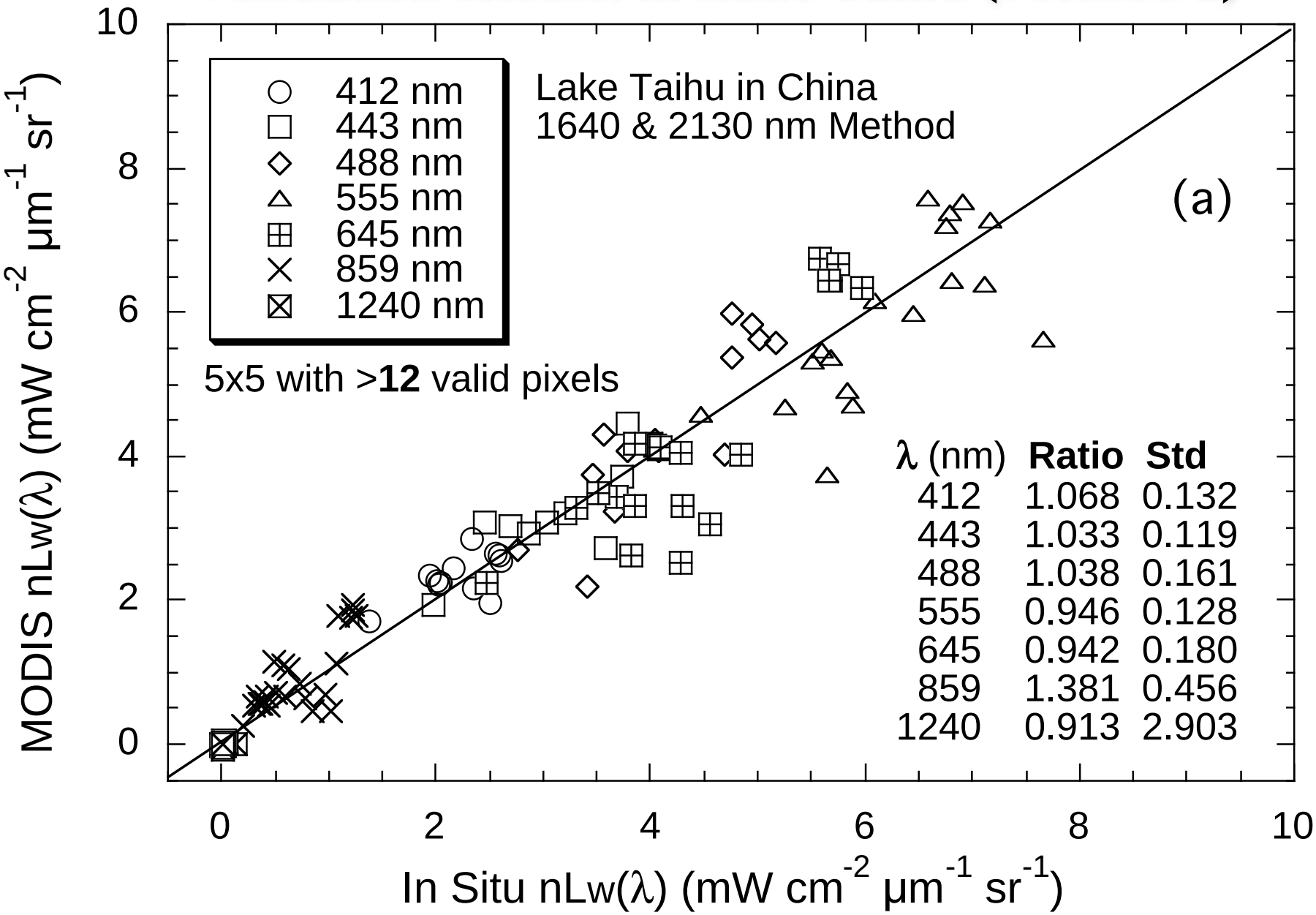

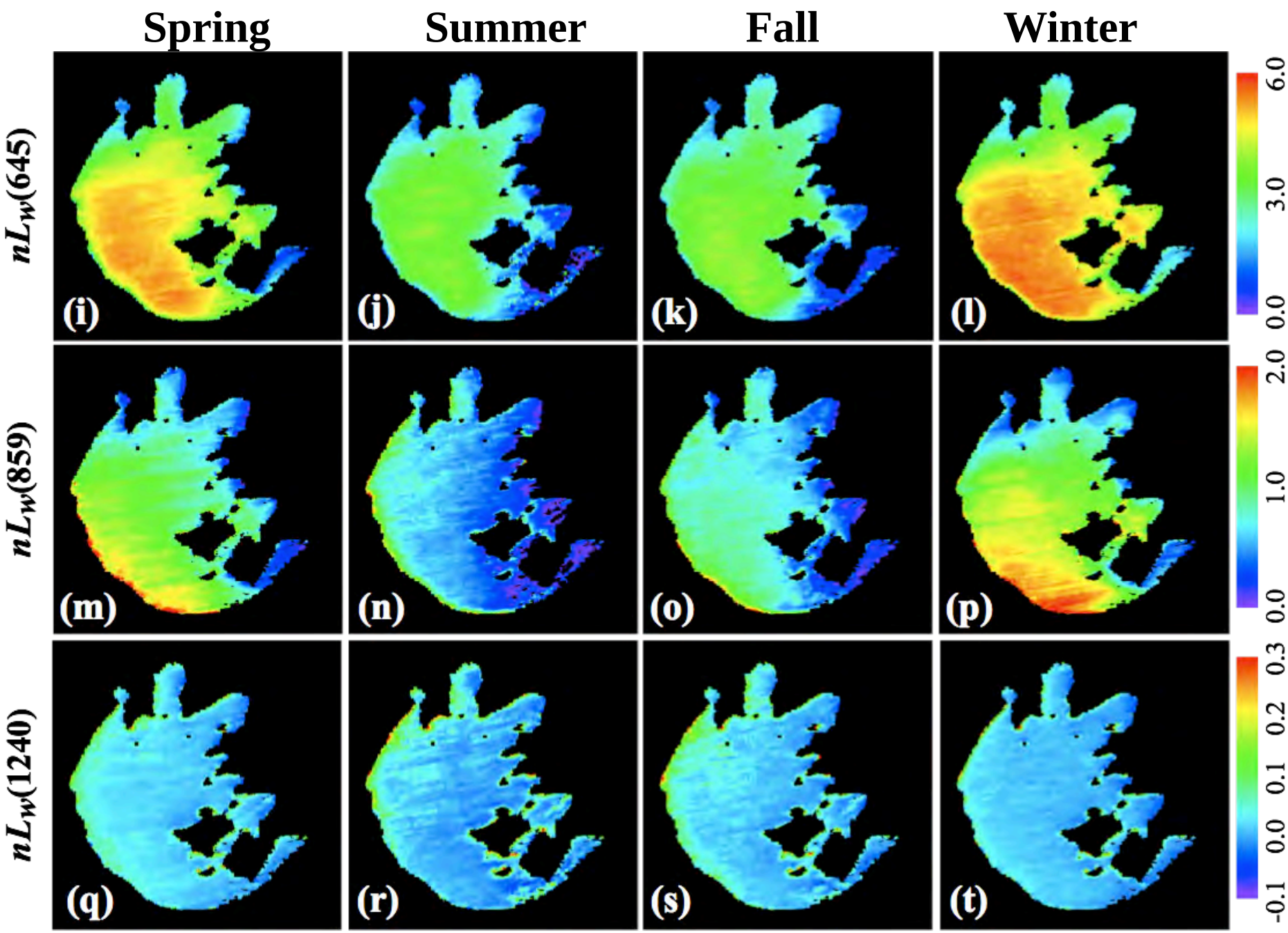
Spring
Summer
Fall
Winter
$nL_w(645)$
$nL_w(859)$
$nL_w(1240)$
(i)
(j)
(k)
(l)
(m)
(n)
(o)
(p)
(q)
(r)
(s)
(t)
6.0
3.0
0.0
2.0
1.0
0.0
0.3
0.2
0.1
0.0
-0.1

Seasonal Histograms in $nL_w(1240)$

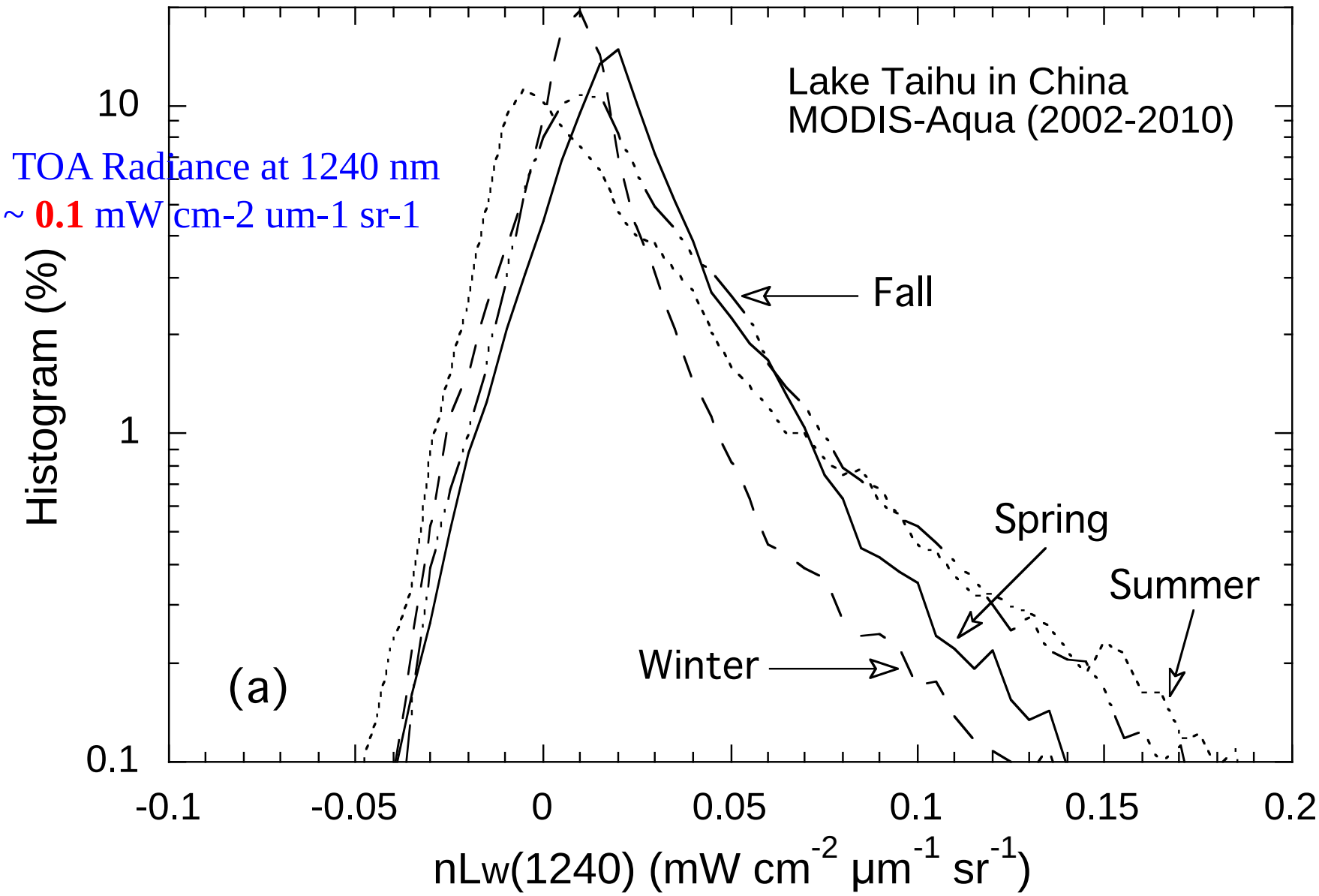

Climatology Histogram in $nL_w(1240)$

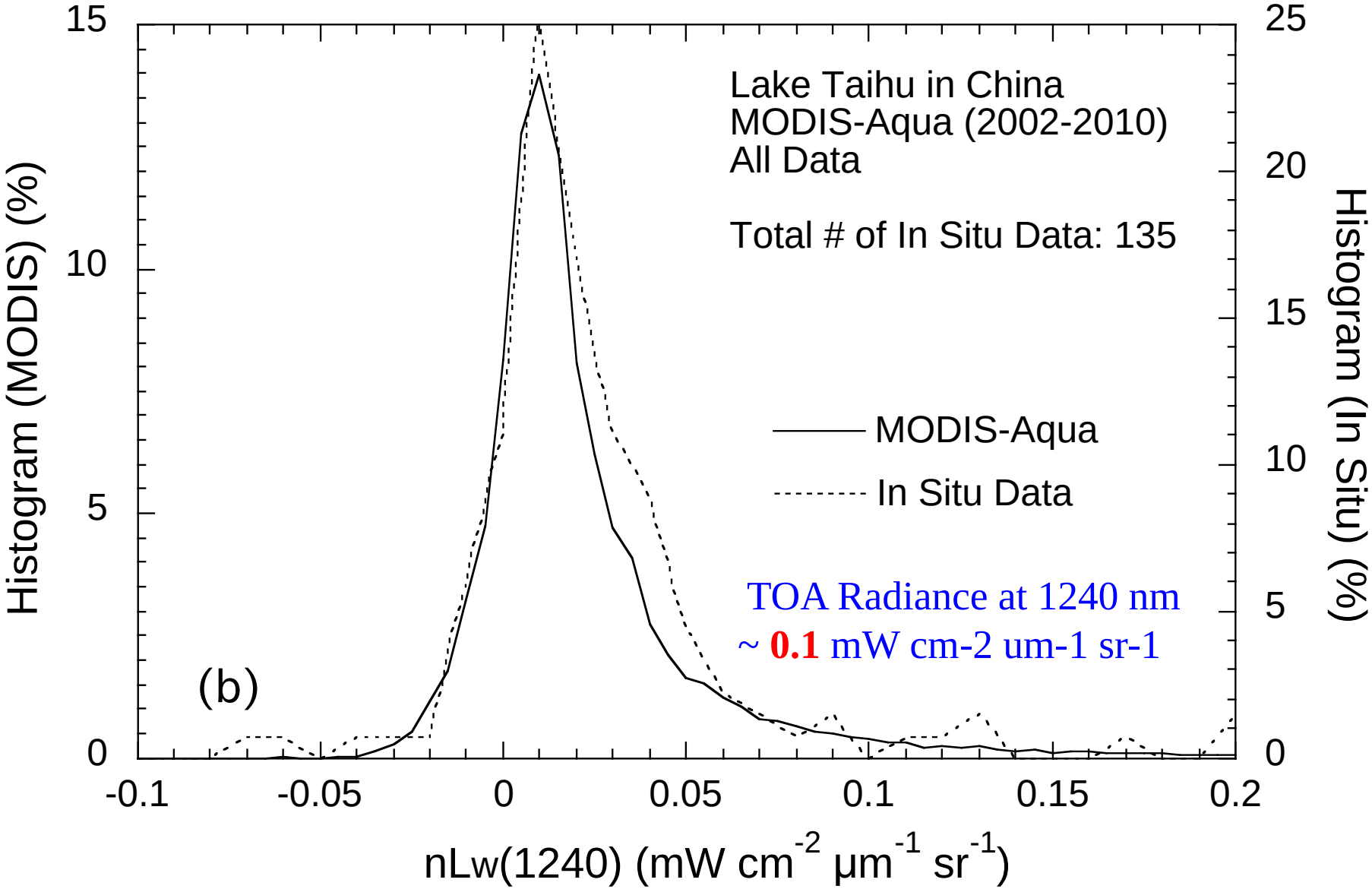

MODIS-Measured Climatology Water Optical Property for Lake Taihu

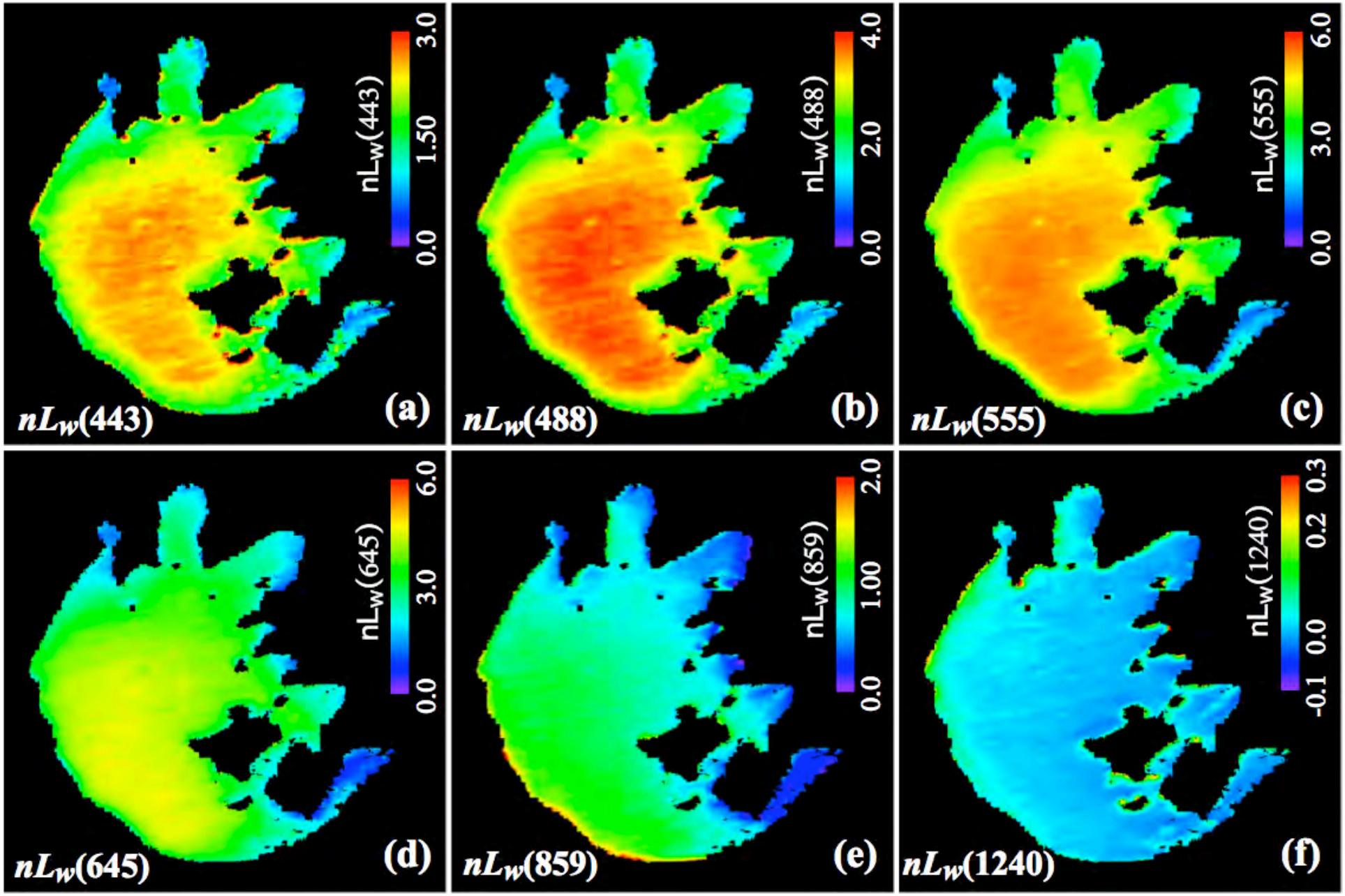

MODIS-Aqua-Derived (2002-2010)
Various Water-leaving Radiance Relationships

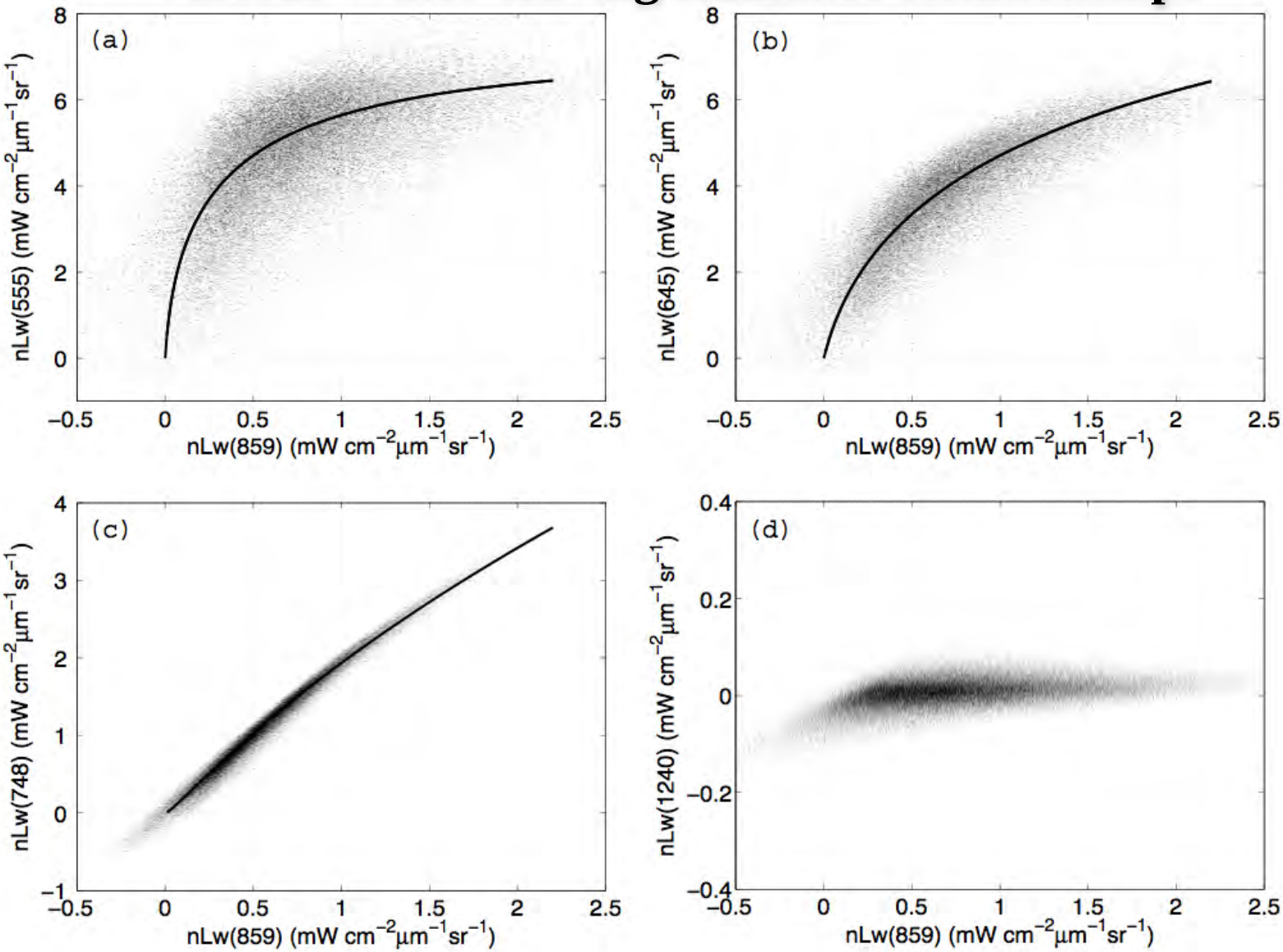

Lake Taihu in China

Radiance Saturation

$$nL_w(\lambda) \sim b_b(\lambda)\, I\, [a(\lambda) + b_b(\lambda)]$$

Radiance saturation phenomenon is attributed to the dominance of $b_b(\lambda)$ for extremely turbid waters, i.e., $b_b(\lambda) >> a(\lambda)$!

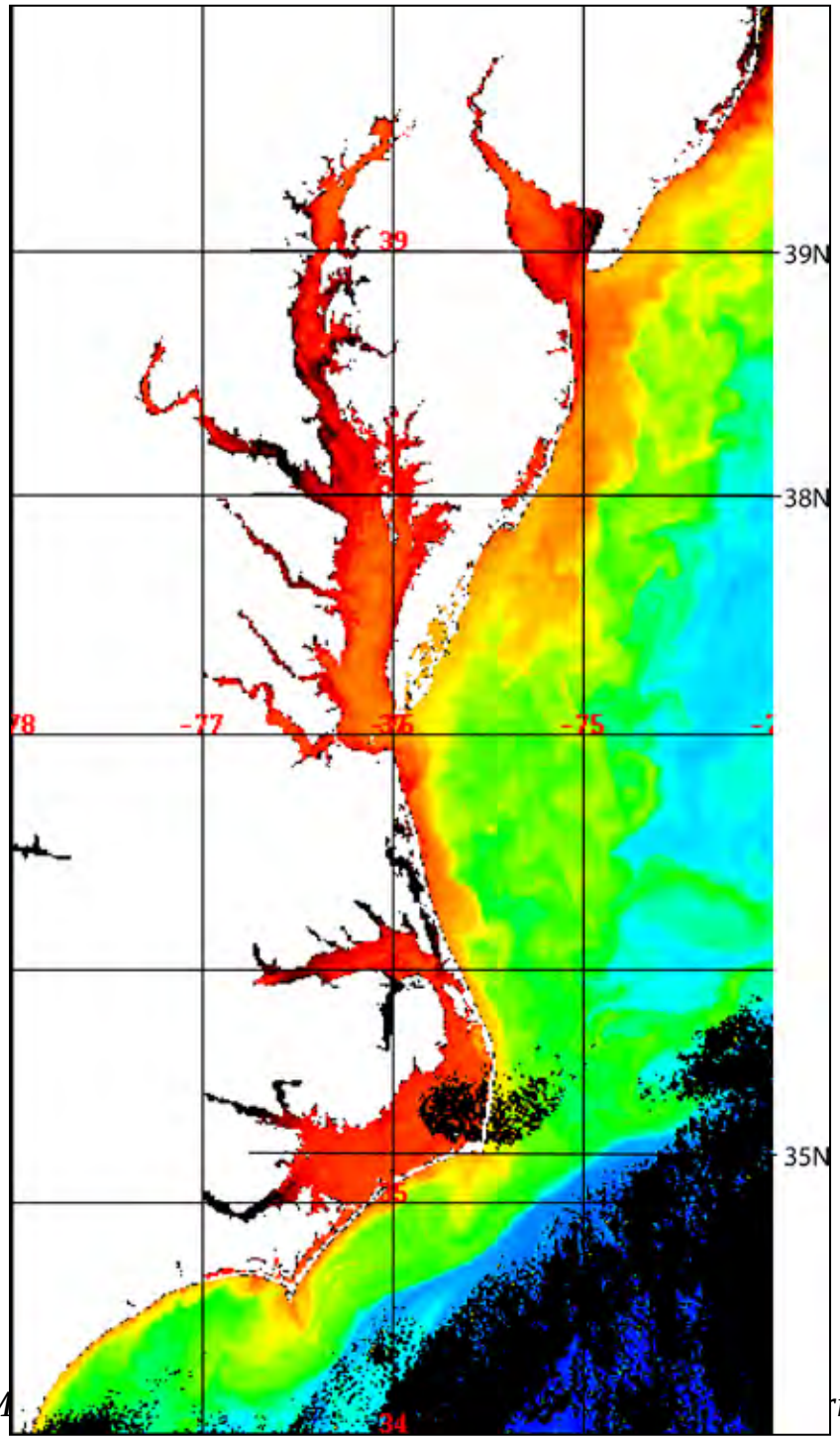

Adjacent Effects on the Ocean Color Products

MODIS-Aqua Mapped Chl-a image in the Chesapeake Bay (Oct. 7, 2004)

A200402811815.L2_LAC

At line 39°N **At line 38°N**

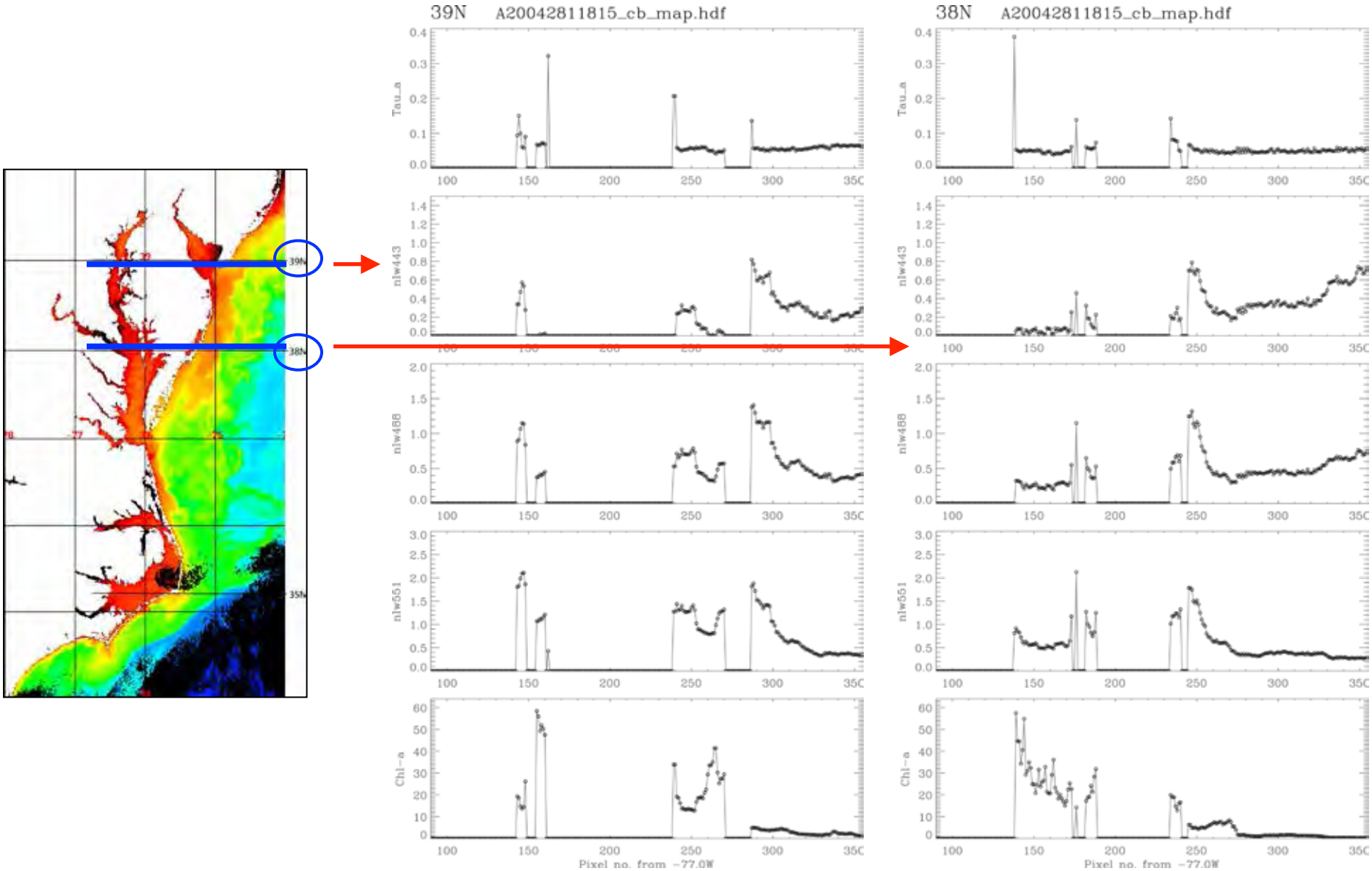

MODIS-NIR

At line 37°N **At line 35°N**

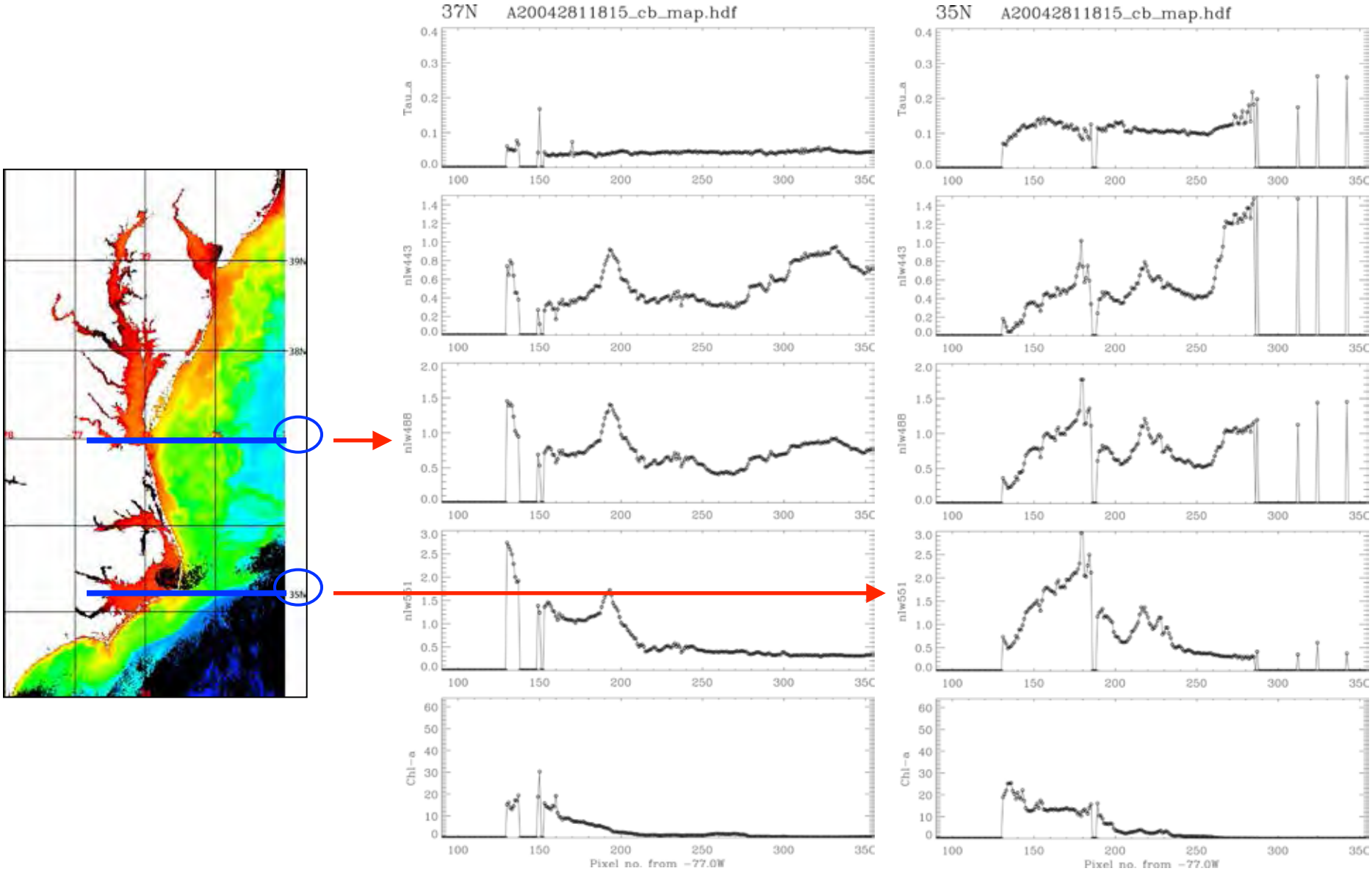

MODIS-NIR

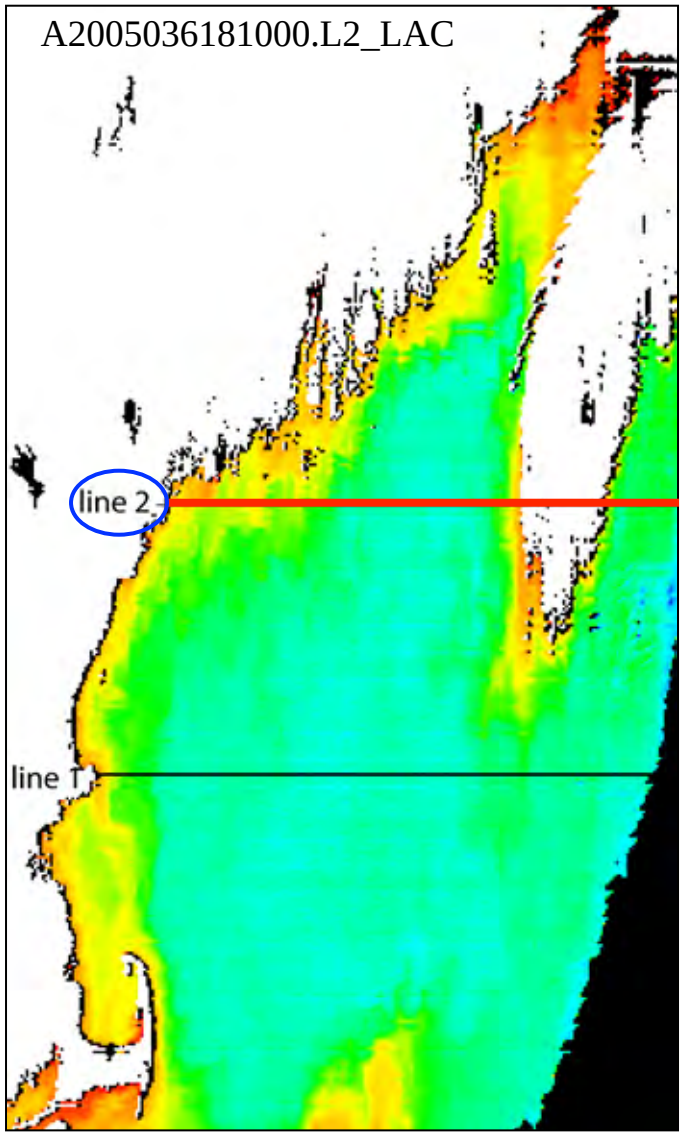

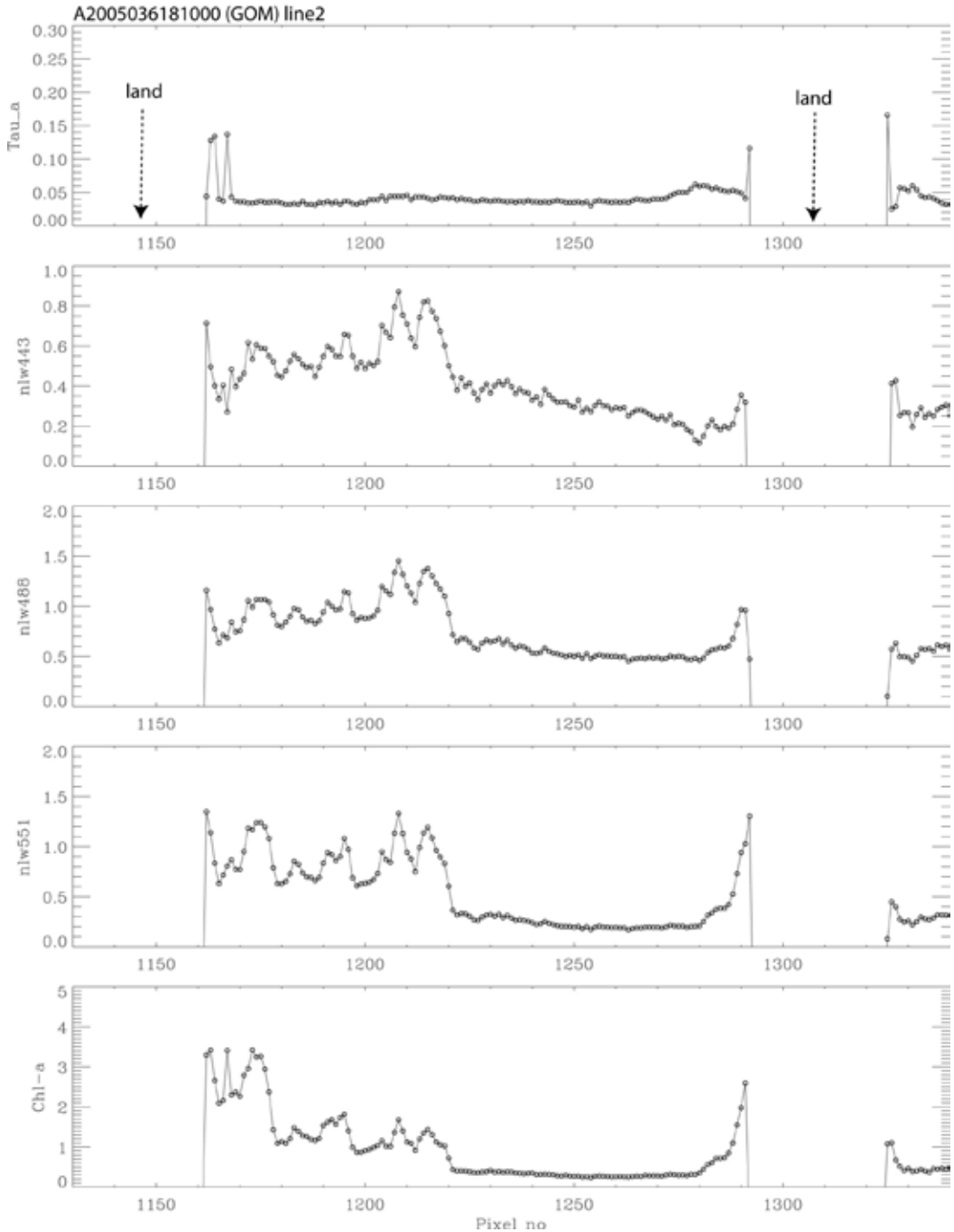

MODIS-Aqua L2 Chl-a image in the Gulf of Maine (Feb. 5, 2005)

The SWIR Algorithm Related Publications (1)
(Algorithms and Validations)

Wang, M. and W. Shi, "Sensor noise effects of the SWIR bands on MODIS-derived ocean color products," *IEEE Trans. Geosci. Remote Sensing* (In press).

Shi, W. and M. Wang, "Sea ice property in the Bohai Sea measured by MODIS-Aqua: 1. Satellite algorithm development," *J. Mar. Syst.*, **95**, 32-40, doi:10.1016/j.jmarsys.2012.01.012, 2012.

Shi, W. and M. Wang, "Sea ice property in the Bohai Sea measured by MODIS-Aqua: 2. Study of sea ice seasonal and inter-annual variability," *J. Mar. Syst.*, **95**, 41-49, doi:10.1016/j.jmarsys.2012.01.010, 2012.

Wang, M., W. Shi, and L. Jiang, "Atmospheric correction using near-infrared bands for satellite ocean color data processing in the turbid western Pacific region," *Opt. Express*, **20**, 741-753, 2012.

Ramachandran, S. and M. Wang, "Near-real-time ocean color data processing using ancillary data from the Global Forecast System model," *IEEE Trans. Geosci. Remote Sensing*, **49**, 1485-1495, 2011.

Zhang, H. and M. Wang, "Evaluations of Sun glitter models using MODIS measurements," *J. Quant. Spectr. Rad. Trans.*, **111**, 492-506, 2010.

Wang, M., S. Son, and L. W. Harding Jr., "Retrieval of diffuse attenuation coefficient in the Chesapeake Bay and turbid ocean regions for satellite ocean color applications," *J. Geophys. Res.*, **114**, C10011, doi:10.1029/2009JC005286, 2009.

Wang, M. and W. Shi, "Detection of ice and mixed ice-water pixels for MODIS ocean color data processing," *IEEE Trans. Geosci. Remote Sensing*, **47**, 2510-2518, 2009.

Shi, W. and M. Wang, "An assessment of the ocean black pixel assumption for the MODIS SWIR bands," *Remote Sens. Environ.*, **113**, 1587-1597, 2009.

Wang, M., S. Son, and W. Shi, "Evaluation of MODIS SWIR and NIR-SWIR atmospheric correction algorithms using SeaBASS data," *Remote Sens. Environ.*, **113**, 635-644, 2009.

Wang, M. and W. Shi, "The NIR-SWIR combined atmospheric correction approach for MODIS ocean color data processing," *Optics Express*, **15**, 15722-15733, 2007.

Wang, M., J. Tang, and W. Shi, "MODIS-derived ocean color products along the China east coastal region," *Geophys. Res. Lett.*, **34**, L06611, doi: 10.1029/2006GL028599, 2007.

Shi, W. and M. Wang, "Detection of turbid waters and absorbing aerosols for the MODIS ocean color data processing," *Remote Sens. Environ.*, **110**, 149-161, 2007.

Wang, M., "Remote sensing of the ocean contributions from ultraviolet to near-infrared using the shortwave bands: simulations," *Appl. Opt.*, **46**, 1535-1547, 2007.

Wang, M. and W. Shi, "Cloud masking for ocean color data processing in the coastal regions," *IEEE Trans. Geosci. Remote Sensing*, **44**, 3196-3205, 2006.

Wang, M. and W. Shi, "Estimation of ocean contribution at the MODIS near-infrared wavelengths along the east coast of the U.S.: Two case studies," *Geophys. Res. Lett.*, **32**, L13606, doi:10.1029/2005GL022917, 2005.

The SWIR Algorithm Related Publications (2)

(Various Applications)

Shi, W. and M. Wang, "Satellite views of the Bohai Sea, Yellow Sea, and East China Sea," *Progress in Oceanography* (In press).

Son, S. and M. Wang, "Water properties in Chesapeake Bay from MODIS-Aqua measurements," *Remote Sens. Environ.*, **123**, 163-174, doi: 10.1016/j.rse.2012.03.009, 2012.

Shi, W., M. Wang, and L. Jiang, "Spring-neap tidal effects on satellite ocean color observations in the Bohai Sea, Yellow Sea, and East China Sea," *J. Geophys. Res.*, **116**, C12932, doi:10.1029/2011JC007234, 2011.

Shi, W., M. Wang, X. Li, and W. G. Pichel, "Ocean sand ridge signatures in the Bohai Sea observed by satellite ocean color and synthetic aperture radar measurements," *Remote Sens. Environ.*, **115**, 1926-1934, 2011.

Shi, W. and M. Wang, "Satellite observations of asymmetrical physical and biological responses to Hurricane Earl," *Geophys. Res. Lett.*, **38**, L04607, doi:10.1029/2010GL046574, 2011.

Wang, M., W. Shi, and J. Tang, "Water property monitoring and assessment for China's inland Lake Taihu from MODIS-Aqua measurements," *Remote Sens. Environ.*, 115, 841-845, 2011.

Son, S., M. Wang, and J. K. Shon, "Satellite observations of optical and biological properties in the Korean dump site of the Yellow Sea," *Remote Sens. Environ.*, **115**, 562-572, 2011.

Shi, W. and M. Wang, "Characterization of global ocean turbidity from MODIS ocean color observations," *J. Geophys. Res.*, **115**, C11022, doi:10.1029/2010JC006160, 2010.

Shi, W. and M. Wang, "Satellite observations of environmental changes from the Tongaa Volcano eruption in the southern tropical Pacific," *Int. J. Remote Sens.*, **32**, 5785-5796, doi: 10.1080/01431161.2010.507679, 2011.

Shi, W. and M. Wang, "Satellite observations of the seasonal sediment plume in central East China Sea," *J. Marine Systems*, **82**, 280-285, 2010.

Son, S. and M. Wang, "Environmental Responses to Land Reclamation Project in South Korea," *Eos, Transaction, American Geophysical Union*, **90**, p398-399, Nov. 3, 2009.

Shi, W. and M. Wang, "Green macroalgae blooms in the Yellow Sea during the spring and summer of 2008," *J. Geophys. Res.*, 114, C12010, doi:10.1029/2009JC005513, 2009.

Shi, W. and M. Wang, "Satellite observations of flood-driven Mississippi River plume in the spring of 2008," *Geophys. Res. Lett.*, **36**, L07607, doi:10.1029/2009GL037210, 2009.

Liu, X, M. Wang, and W. Shi, "A study of a Hurricane Katrina-induced phytoplankton bloom using satellite observations and model simulations," *J. Geophys. Res.*, **114**, C03023, doi:10.1029/2008JC004934, 2009.

Shi, W. and M. Wang, "Three-dimensional observations from MODIS and CALIPSO for ocean responses to Cyclone Nargis in the Gulf of Martaban," *Geophys. Res. Lett.*, **35**, L21603, doi:10.1029/2008GL035279, 2008.

Nezlin, N. P., P. M. DiGiacomo, D. W. Diehl, B. H. Jones, S. C. Johnson, M. J. Mengel, K. M. Reifel, J. A. Warrick, and M. Wang,"Stormwater plume detection by MODIS imagery in the southern California coastal ocean," *Estuarine, Coastal and Shelf Science*, **80**, 141-152, 2008.

Wang, M. and W. Shi, "Satellite-observed blue-green algae blooms in China's Lake Taihu", *Eos, Transactions, American Geophysical Union*, 89, p201-202, May 27, 2008.

Shi, W. and M. Wang, "Observations of a Hurricane Katrina-induced phytoplankton bloom in the Gulf of Mexico," *Geophys. Res. Lett.*,**34**, L11607, doi:10.1029/2007GL029724, 2007.

Questions?